

**Nondestructive evaluation of larval
development and feeding behavior of
the bamboo powderpost beetle
Dinoderus minutus in bamboo culms**

Hiroki WATANABE

2018

Contents

General introduction.....	1
Chapter 1. Literature review and objectives.....	5
1.1. Introduction	5
1.2. Insect pests of bamboo culms in Japan.....	5
1.3. Studies on the biology and control of <i>D. minutus</i> and closely related species	9
1.4. Nondestructive techniques for detecting insects and insect attack in wood	11
1.5. Objectives	15
Chapter 2. Evaluation of larval development and feeding behavior using X-ray computed tomography	16
2.1. Introduction	16
2.2. Visualization of larval growth process and tunneling process in infested bamboo culms	17
2.2.1. Materials and methods.....	17
2.2.2. Results and discussion on larval growth and tunneling observed in CT images	19
2.3. Evaluation of individual egg-to-adult development and feeding behavior	25
2.3.1. Egg collecting.....	25
2.3.2. Inoculation of larvae in bamboo and X-ray CT scanning.....	27
2.3.3. Results and discussion on larval–pupal development and larval feeding.....	30
2.3.4. Discussion on larval duration	35
2.3.5. Pre-mating adult feeding	37
2.4. Summary	39
Chapter 3. Relationship between the movements of the mouthparts and the generation of acoustic emission	41
3.1. Introduction	41
3.2. Materials and methods.....	42
3.2.1. Experimental insects and bamboo specimens.....	42
3.2.2. Apparatuses	44
3.2.3. Measurement of time lags between AE signals and video signals	46
3.2.4. Analysis	47
3.3. Results and discussion.....	48
3.3.1. Larval feeding.....	48
3.3.2. Adult feeding	55
3.4. Summary	57

Chapter 4. Combined use of acoustic emission and X-ray computed tomography to monitor larval feeding activity and development	58
4.1. Introduction	58
4.2. Materials and methods.....	59
4.2.1. Preparation of bamboo pieces and inoculation of larvae	59
4.2.2. AE measurement and analysis	61
4.2.3. Direct observation of ecdysis and pupation (Additional experiment I).....	62
4.2.4. Measurement of distance attenuation of elastic waves in bamboo (Additional experiment II).....	63
4.2.5. Measurement of amplitude of AE generated by larvae of different instars (Additional experiment III)	64
4.2.6. Estimation of head capsule widths of all instars (Additional experiment IV).....	65
4.3. Results and discussion.....	66
4.3.1. Feeding activity and development from the first instar to adult eclosion.....	66
4.3.2. Effects of attenuation of AE waves	74
4.3.3. Relationship between cumulative AE hits and bamboo consumption.....	79
4.3.4. Pre-mating adult feeding activity.....	81
4.4. Summary	82
Chapter 5. General discussion and future perspectives	84
5.1. Introduction	84
5.2. Novelty of monitoring using X-ray CT and AE in entomology	84
5.3. Usefulness of X-ray CT and AE monitoring in managing <i>D. minutus</i>	86
5.3.1. Desirable process of IPM for bamboo materials	86
5.3.2. Application of X-ray CT and AE to inspection of insect attack	88
5.3.3. Application of X-ray CT and AE as laboratory analysis tools in developing control measures.....	89
Summary and conclusions.....	93
Acknowledgements	95
References	96

General introduction

In many temperate and tropical regions of the world, bamboo species (family Poaceae: subfamily Bambusoideae) are an abundant natural resource because of their fast-growing nature (Fujii 2013, Uchimura 2005, 2009, 2012). They produce culms, in which hollow internodes are separated by diaphragms at the nodes. Bamboo culms are flexible and have highly useful mechanical properties (Fujii 2013, Uchimura 2005, 2009, 2012). For example, the tensile strengths of culms of madake, *Phyllostachys bambusoides*, and moso bamboo, *P. edulis* (syn.: *P. pubescens*), the two most common bamboo species in Japan, are 270% and 190%, respectively, of sugi (*Cryptomeria japonica*) wood, and the compression strengths of madake and moso bamboo culms are both 210% of sugi wood (Forestry and Forest Products Research Institute 2004). Bamboo culms also exhibit high machinability and desirable aesthetic qualities (Fujii 2013, Okahisa *et al.* 2005, Uchimura 2005, 2009, 2012). In Japan, bamboo culms have been used to make household goods, such as furniture products, tools, and utensils, and craft products, and as materials for agricultural and forestry uses (Fujii 2013, Uchimura 2005, 2009, 2012, Ueda 1963). In wooden buildings, they have also been used mainly as decorative elements and as a lathing material for clay walls (Fujii 2013, Uchimura 2005, 2009, 2012, Ueda 1963). However, primarily because of the spread of alternative materials such as plastics and metals, the demand for bamboo culms has been decreasing in Japan (Forestry Agency 2011, Uchimura 2005, 2009, 2012). For example, the production quantity and import of bamboo culms decreased by 35% and 57%, respectively, between 1998 and 2009 (Forestry Agency 2011). The decreasing demand for bamboo has led to expanding areas of bamboo forests being left abandoned, which is being taken up as an environmental issue (Forestry Agency 2011, Uchimura 2009).

A major reason for bamboo materials being replaced by alternatives is their lack of durability. Bamboo culms are known to be susceptible to biodeterioration and are readily attacked by insect pests (Fujii 2013, Okahisa *et al.* 2005), which can reduce the strength and aesthetic values of the culms. Susceptibility to insect attack is an unavoidable problem in attempts to reinvigorate the demand of bamboo culms not only as materials for conventional uses but also for novel uses, especially as construction materials, taking advantage of their strength qualities.

There are two possible ways for insect infestation to occur in bamboo culms. Adult insects may enter and oviposit in bamboo culms during the processes of felling, seasoning, and processing, and the infected culms may be made into products or integrated into constructions without being detected. Adults may also enter bamboo products or materials in use, where they subsequently reproduce and cause damage. To eliminate the former route of infestation, preventive measures are necessary. When insect entrance and oviposition are suspected, remedial treatments, such as the use of insecticides or heat treatment, are also needed. Preventive and remedial measures that do not rely heavily on chemicals are desirable because of the associated impacts on the environment and human health. The latter route of infestation can be dealt with by regular inspection to detect insect attack at an incipient stage. Development of accurate and practical detection systems to inspect for insect damage is necessary. Damaged parts should be processed using a remedial treatment or be disposed of and replaced. The application of preventive measures to treated or replacing parts is necessary to prevent re-infestation.

Establishment of integrated pest management (IPM) with a combination of protection, remediation, and inspection measures requires nondestructive techniques that can be used to detect and analyze insect activities in bamboo culms. Such

techniques could be useful in evaluating the efficacy of preventive and remedial measures, and the principles of the technology could be applied to the development of practical *in situ* detection apparatuses. Furthermore, such techniques could also be used in laboratory studies to monitor the activities of individual insects, revealing fundamental information regarding the biology of bamboo-boring insects, on which any aspect of IPM should be based.

Knowledge regarding the life history, such as developmental periods of all stages, the number of larval instars, and the reproductive capacity of adults, is important. Information on developmental periods can be used to estimate the occurrence of infestation. Determining instars is important in implementing remedial treatments because the effects of such treatments may differ depending of the developmental stages including instars. Information related to insect damage, such as the temporal and spatial patterns of tunneling, is also useful for estimating the extent of damage and reduced strength by inspection and for modeling the progress of damage. However, as revealed in Chapter 1, reliable information regarding the development and feeding of even the most important insect pest, the bamboo powderpoest beetle *Dinoderus minutus*, in bamboo culms is scarce, and applicability of any nondestructive technique to reveal such information is yet to be investigated.

The primary purpose of this research was to find nondestructive techniques suitable for obtaining fundamental knowledge on *D. minutus* that is necessary for establishing IPM strategies. Because the larval stages are the most difficult to analyze, this research particularly focused on larval development and feeding. The applicability of two nondestructive techniques, X-ray computed tomography (CT) and acoustic emission (AE) monitoring was tested.

This doctoral thesis consists of five chapters. In Chapter 1, existing literature

on the biology and control of bamboo-boring insects, particularly *D. minutus*, is reviewed. Then, literature on methods for nondestructive detection and inspection of insect attack in wood is reviewed in order to search for appropriate techniques to investigate larval development and feeding characteristics of *D. minutus*. Based on this review of the literature, the objectives of this research are clarified.

In Chapters 2–4, experiments conducted to evaluate the applicability of X-ray CT and AE monitoring are described. In Chapter 2, the applicability of X-ray CT for quantitatively evaluating the processes of larval growth and feeding is discussed. In Chapter 3, the relationship between the movements of the mouthparts, particularly mandibles, of *D. minutus* and the generation of AE is clarified, and the effectiveness of AE monitoring for the continuous analysis of feeding activity is proposed. In Chapter 4, the use of continuous AE monitoring of feeding activity to determine the number and time periods of instars and to analyze the rhythmic patterns of feeding is described. The relationships among the transitions of feeding activity, larval development, and the amount of bamboo consumed by the larvae are also discussed based on the combined use of X-ray CT and AE monitoring. Finally, in Chapter 5, the entomological significance of X-ray CT and AE monitoring and the findings obtained using these techniques is summarized, and applicability and future perspectives of the techniques and findings for IPM for bamboo materials are discussed.

Chapter 1. Literature review and objectives

1.1. Introduction

In this chapter, the literature on insect pests of bamboo culms in Japan and the biology and control of the bamboo powderpost beetle *Dinoderus minutus* is reviewed. Then, literature on nondestructive methods for detecting insect attack in wood is reviewed in order to search for appropriate techniques to investigate larval development and feeding characteristics of *D. minutus* in bamboo culms. Based on this review, the objectives of this research are clarified.

1.2. Insect pests of bamboo culms in Japan

In Japan, notable insect species that attack bamboo culms after felling belong to two families, Bostrichidae and Cerambycidae, of beetles (order Coleoptera). Bamboo pests in the former family include the bamboo powderpost beetle *D. minutus*, the Japanese shot-hole borer *D. japonicus*, the brown powderpost beetle *Lyctus brunneus*, and the oriental powderpost beetle *Lyctoxylon dentatum* (Mori and Arai 1979, The Society of House and Household Pests Science, Japan 1995, Tokyo National Research Institute for Cultural Properties 2001, Ueda 1963, Wood Technological Association of Japan 1961, Yamano 1976, Yasutomi and Umeya 1983). The genus *Dinoderus* is classified in subfamily Dinoderinae, and the genera *Lyctus* and *Lyctoxylon* in subfamily Lyctinae. In the latter family (Cerambycidae), two species, *Purpuricenus temminckii* and *Chlorophorus annularis*, are known as common pests of bamboo (Mori and Arai 1979, The Society of House and Household Pests Science, Japan 1995, Tokyo National Research Institute for Cultural Properties 2001, Ueda 1963, Wood Technological Association of Japan 1961). Termite species are not known as major pests of bamboo,

although species such as *Reticulitermes speratus* and *Coptotermes formosanus* can attack bamboo culms (The Society of House and Household Pests Science, Japan 1995).

Among these species, *D. minutus* is considered to be the most important bamboo pests in Japan (Mori and Arai 1979, The Society of House and Household Pests Science, Japan 1995, Wood Technological Association of Japan 1961, Yamano 1976, Yasutomi and Umeya 1983), as well as being a cosmopolitan species throughout tropical and temperate regions (Fisher 1950). Therefore, this species was chosen as the test species in this research.

General information regarding the biology and attack of *D. minutus* can be summarized as follows based on literature in Japan, including books and encyclopedia (Mori and Arai 1979, The Society of House and Household Pests Science, Japan 1995, Tokyo National Research Institute for Cultural Properties 2001, Ueda 1963, Wood Technological Association of Japan 1961, Yamano 1976, Yasutomi and Umeya 1983). Adults of *D. minutus* are dark brown beetles with a body length of 2.5–3.5 mm. Mated adults enter bamboo culms from cut surfaces, create tunnels, and oviposit inside. The hatched larvae develop by boring into and feeding on the parenchyma near the inner surface of culms. Larvae are known to undergo five instars. After completing the larval stages, they pupate inside the culms. The adults also feed on bamboo after adult eclosion and leave via an exit hole. In the process of oviposition and larval and adult feeding, they turn bamboo culms into frass, a powdery mixture of excrement and bamboo fragments. Tunnels bored by larvae are packed with frass, while adults discharge frass from their tunnels. Piles of frass resulting from adult tunneling can be a sign of infestation. *Dinoderus minutus* has one to four broods per year, and adults are seen from March to November. They hibernate in both larval and adults stages. It is considered that starch stored in bamboo parenchyma attracts the beetles. Because the

starch content in bamboo culms fluctuates throughout the year, it is traditionally recommended to fell culms in particular seasons of the year, generally said to be from fall to winter, to reduce susceptibility. *Dinoderus minutus* has been recorded as infesting a historical house conserved as a cultural property, where bamboo ceiling of the house was severely damaged and adults that fell from the ceiling caused further damage to the tatami mats.

Other than attacking bamboo materials, *D. minutus* may also infest non-woody materials such as stored crops (Nobuchi 1986, 1992). Infestation of *D. minutus* in Susuki grass, *Miscanthus sinensis*, stored as a roofing material for a Japanese shrine was reported previously (Fukuda *et al.* 1994). Adults are known to bore into materials that are not suitable for reproduction, for example, softwoods, hardwoods, and even non-plant materials such as telecommunication cables (Miyamoto 1985, Nobuchi 1986, 1992, The Society of House and Household Pests Science, Japan 1995, Wood Technological Association of Japan 1961). The reasons for this type of behavior may include feeding and hiding (Nobuchi 1992) but as yet they remain unclear. In addition, infestation of *D. minutus* may accompany the occurrence of a parasitoid bethylid wasp, *Sclerodermus nipponicus*, which is known as a stinging pest (Tokyo National Research Institute for Cultural Properties 2001).

The morphology of adult *D. minutus* is very similar to other *Dinoderus* spp. found in Japan. The antennae of *D. minutus* are 10-segmented, which can be used to differentiate *D. minutus* from *D. japonicus* that have 11-segmented antennae (Fisher 1950, Mori and Arai 1979, Nobuchi 1986, 1992, The Society of House and Household Pests Science, Japan 1995, Tokyo National Research Institute for Cultural Properties 2001, Ueda 1963, Wood Technological Association of Japan 1961, Yamano 1976). Compared with *D. minutus*, *D. japonicus* is slightly larger and slightly darker in color,

though attacks may be more occasional and it is known to have only one brood per year (Mori and Arai 1979, Nobuchi 1986, 1992, The Society of House and Household Pests Science, Japan 1995, Tokyo National Research Institute for Cultural Properties 2001, Ueda 1963, Wood Technological Association of Japan 1961). Two other species of *Dinoderus* have been identified in Japan, *D. bifoveolatus* and *D. speculifer* (Nobuchi 1986, 1992). The former species has 12–14 denticles on the anterior edge of the pronota and elytra with ocellate punctures, whereas *D. minutus* has 8–10 denticles and elytra without ocellate punctures (Fisher 1950, Nobuchi 1986, 1992, Schäfer *et al.* 2000). This species was first recorded in Japan by Nobuchi (1986), and there are several subsequent records (City of Nagoya 2009, Kawakami and Iwata 1993), but it is not known to have become established in Japan. It attacks hardwoods and palm timbers (Nobuchi 1986, 1992, The Society of House and Household Pests Science, Japan 1995). The latter species, *D. speculifer*, is darker and larger than *D. minutus* and *D. bifoveolatus* and has 12–14 denticles on the anterior edge of the pronota (Nobuchi 1986). It is a rare species and the host materials are unknown (Nobuchi 1986). The pronota of *D. ocellaris*, another bamboo borer found in India and some other parts of Asia, are not distinctly bifoveolate, unlike *D. minutus* and some other *Dinoderus* spp. (Fisher 1950), but this species has not been found in Japan.

According to Abood *et al.* (2010), adults of *D. minutus* do not have apparent morphological sexual characteristics, with the body size not significantly different between males and females. However, they reported that sexes can be easily differentiated in the pupal stage based on morphological differences of the last abdominal segments.

1.3. Studies on the biology and control of *D. minutus* and closely related species

Being an important pest of bamboo in many countries, studies on *D. minutus* have been conducted by some researchers who have sought to clarify the biology of this species and to develop effective control measures. Plank (1948) described the life history of *D. minutus* in Puerto Rico. For the examination of larval stages, he used culms of *Bambusa vulgaris* as a rearing medium and observed the larvae by chipping the culms into sections with a small knife. He found four larval instars based on Dyar's (1890) rule, although each instar period could not be measured. Plank (1950) investigated factors influencing the susceptibility of culms of several bamboo species to adult *D. minutus* and found that the starch content was the most important. Plank and Hageman (1951) conducted a more quantitative analysis of starch content and reported a strong positive correlation between the starch content in bamboo culms and the susceptibility to attack by adult *D. minutus*. Nair *et al.* (1983) described the attack of *Dinoderus* spp. on *Ochlandra travancorica* culms in India and showed the suitability of tapioca and wheat flour based diets for laboratory culture of *D. minutus*. Another study on artificial diets was conducted by Suzuki and Kirton (1991), and flour cakes of some cereals such as whole wheat and buckwheat were found to be suitable.

The efficacy of chemical treatments to increase the resistance of bamboo has also been investigated. Ninomiya and Kotani (2002) showed that acetylation of madake (*Phyllostachys bambusoides*) culms could prevent the entrance of adult *D. minutus* beetles. Treatment with insecticides such as thiamethoxam (Acda 2008), deltamethrin, and permethrin (Garcia and Morrell 2010) was also proven to effectively protect *B. vulgaris* culms from feeding and oviposition of *D. minutus*.

Recently, further findings on the life history and characteristics of attack have

been reported. Garcia and Morrell (2008) monitored the field abundance of *D. minutus* throughout different seasons in the Philippines and showed that factors such as starch content in *B. vulgaris* culms and temperature influenced the populations. Garcia and Morrell (2009) estimated the developmental threshold temperatures and thermal requirements of egg, larval, and pupal stages of *D. minutus* in the Philippines based on the developmental periods of these stages at different temperatures. Larval development in *B. vulgaris* culms was observed using a razor blade for dissection. Norhisham *et al.* (2013) used an individual rearing method, which was adapted from the method of Iwata and Nishimoto (1985) for studies of *L. brunneus* (see the following paragraph), to investigate larval development of *D. minutus* in Malaysia. They used cassava flour as a rearing medium and found five larval instars based on the inspection of exuviae. Abood and Norhisham (2013) used cassava pellets as an oviposition medium to determine the effects of humidity on the reproductive capacity and egg hatchability of *D. minutus* in Malaysia. Although the number of eggs laid by females increased with relative humidity, egg hatchability decreased when relative humidity was high (85%). Norhisham *et al.* (2015) investigated the effects of moisture content in *Gigantochloa scortechinii* culms on the boring capacity and life span of adult *D. minutus* in Malaysia. At optimum moisture content, 15%, the developmental periods of egg, larvae, and pupae in *G. scortechinii* culms were measured. Inspection of larvae was carried out with a dissection knife.

In addition, literature on methodologies for investigating the life history, especially larval development, of other species closely related to *D. minutus* was reviewed. Sitaraman (1951) described the life history of *D. ocellaris*. Rearing in maize powder was used for the investigation of larval period, and molting was confirmed by microscopic observation of exuviae. Wright (1960) designed cages, each made of wood

flour filled between a pair of glass panes or slides, to observe the movement and development of the southern lyctus beetle, *L. planicollis*, but the wood flour was not thin enough, although 1 or 2 mm thick, to observe the larvae, and no larvae survived until pupation. Iwata and Nishimoto (1985) developed an individual rearing method to study the larval development of *L. brunneus*. This method utilized gelatin capsules containing stuffed buckwheat flour as a diet and single larvae. Ecdysis events were detected by microscopic inspection of exuviae in the material that remained on a sieve.

Review of the literature on *D. minutus* revealed that, although factors influencing the susceptibility of bamboo culms and treatments to increase resistance have been investigated in several studies based on the visible behavior of adults, no reliable methods to analyze the feeding of larvae have been established. Biological studies on the larval development of *D. minutus* have relied on the direct dissection of bamboo culms, which may have affected the natural development or behavior of the larvae, or on tests using artificial diets, in which the larval development or behavior may be different from those in bamboo culms. The same was true for other related species. In addition, there are no reliable reports on the extent of attack caused by *D. minutus* larvae. Therefore, techniques to nondestructively analyze larval development and feeding are desired. In the next section, literature on methods for nondestructive detection and analysis of insects in wood is reviewed in order to search for appropriate approaches for the analysis of *D. minutus*.

1.4. Nondestructive techniques for detecting insects and insect attack in wood

The cryptic nature of xylophagous insects has hindered studies regarding their biology and control in the fields of forest and wood sciences. Many studies have been

made on techniques to detect, visualize, or monitor the presence and attack of insects in logs, timber, wooden products, and wooden constructions in order to either study the biology of insects or inspect for insect damage.

One such technique is the use of X-rays. Radiography, or roentgenography, is a technology that images the internal structure of an object on the principle that the amount of X-ray absorption in the object depends on its density and composition. Radiography has been able to not only visualize insect tunnels and presence but also determine the developmental stages, estimate population size, and trace the growth process of insects inside wood (Amman and Rasmussen 1969, Berryman and Stark 1962, Fisher and Tasker 1940, Jones and Ritchie 1937, Mori *et al.* 1979, Yaghi 1924). Jones and Ritchie (1937) confirmed spectrographically that the larvae of *Lyctus* sp. had greater absorption of X-rays than wood owing to the concentration of mineral salts present in wood. However, only thin plates of wood could be used to trace the movement or growth of insects. The development of X-ray computed tomography (CT) has eliminated this limitation. In X-ray CT, either the object or the pair of the X-ray source and detector is rotated so that a stack of cross-sectional images of the object can be obtained through reconstruction. X-ray CT was used to visualize the tunnels or galleries of the oak platypodid beetle *Platypus quercivorus* (Sone *et al.* 1995), a xiphytriid woodwasp *Rhysacephala warraensis* (Jennings and Austin 2011), the whitespotted sawyer *Monochamus scutellatus* (Bélanger *et al.* 2013), and drywood termite species *Cryptotermes secundus* (Fuchs *et al.* 2004) and *Incisitermes minor* (Himmi *et al.* 2014, Yanase *et al.* 2014) developed in wood blocks or logs. Larval bodies of an anobiid beetle *Priobium cylindricum* were also captured in X-ray CT images (Kigawa *et al.* 2009, Torigoe *et al.* 2010). Although it may not be useful to trace the movement of certain individual termites because of their active locomotion and

aggregation behavior, it is considered promising for tracing larvae of *D. minutus*, which are probably more quiescent in terms of locomotion.

Different types of technique for *in situ* nondestructive detection of wood-attacking insects, most importantly termites, have been developed. Acoustic emission (AE) is a typical example. AE is a phenomenon in which elastic waves are generated by the release of the stored strain energy when local material changes, such as microfractures, occur. Elastic waves released by this phenomenon are called AE waves, and material changes resulting in the generation of AE waves are called AE events. Although there are no specified frequency ranges for the definition of AE waves, practically, frequencies in the ultrasonic range are utilized and, in the studies reviewed below, AE sensors with resonant frequencies of 50–150 kHz were most commonly used. Early studies showed that detectable AE waves were generated by active infestation of termites in wood, and the characteristics of termite-related AE waves were investigated (Fujii *et al.* 1990, Lemaster *et al.* 1997, Lewis and Lemaster 1991, Lewis *et al.* 1991, Noguchi *et al.* 1991, Robbins *et al.* 1991, Scheffrahn *et al.* 1993). Direct observation of termite behavior and simultaneous AE measurement confirmed that AE waves were generated by the feeding activity of termites (Fujii *et al.* 1995, Matsuoka *et al.* 1996). Investigations were made to design suitable sensor types and waveguide types and to build portable detection devices (Lewis *et al.* 2004, Scheffrahn *et al.* 1993, Yanase *et al.* 1998, 1999, 2000a, 2000b, 2001). AE monitoring was successfully applied to termite detection in wooden constructions (Fujii *et al.* 1998, Weissling and Thoms 1999, Yanase *et al.* 1999, 2001) and bait traps (Fujii *et al.* 1997). It was also applied to biological analyses of feeding responses of termites to different conditions (Imamura and Fujii 1995, Indrayani *et al.* 2003, 2007a, 2007b), suggesting that it was an effective tool for biological studies of wood-attacking insects. Furthermore, some studies dealt with AE

generated by wood-boring beetles, such as *Lyctus* spp. (Creemers 2015, Fujii *et al.* 1992, Imamura *et al.* 1998), cerambycid beetle species *Semanotus japonicus* (Fujii *et al.* 1992, 1994) and *Hylotrupes bajulus* (Creemers 2013, 2015), and anobiid beetle species *Anobium punctatum*, *Xestobium rufovillosum* (Creemers 2013, 2015), and *Oligomerus ptilinoides* (Le Conte *et al.* 2015). These previous reports suggested that the feeding activity of *D. minutus* should generate AE waves, and the detection of AE waves could allow continuous analysis of their feeding, which is closely related to larval growth and development.

Another example of *in situ* detection is the detection of odor or gases emitted by insects. The olfactory ability of trained dogs to find termite infestation was tested and shown to be accurate enough for practical use (Brooks *et al.* 2003, Lewis *et al.* 1997). Development of gas sensors to detect odor and metabolic gases emitted by termites was also pursued (Yanase *et al.* 2012, 2013a, 2013b). Termites are known to emit gases, such as carbon dioxide, methane, and hydrogen through metabolism (Khalil *et al.* 1990, Sanderson 1996, Sugimoto *et al.* 1998, Zimmerman *et al.* 1982), and among sensors designed to target these gases, the hydrogen sensor was found most suitable for termite detection (Yanase *et al.* 2012, 2013a, 2013b). In addition, the feasibility of detection of insects, including beetles, in art objects by measurements of respiration, i.e., measurements of concentration changes of carbon dioxide (Koestler *et al.* 2000) and oxygen (Stušek *et al.* 2000), was proposed. In the present research, however, methods of chemical detection were not used for detection and analysis of *D. minutus* because bostrichid beetles are not known to emit special metabolic gases and measurement of respiration may require sensors with high sensitivities to detect changes in carbon dioxide and oxygen levels in the atmosphere. Gas detection may perhaps be a promising approach to analyze anobiid or cerambycid beetles which are known to digest cellulose

or hemicellulose with the aid of gut microorganisms (Yoshimura 2016).

Techniques using electromagnetic waves to detect moving termites were also developed. Termite movement in wood could be detected by measuring the reflected components of microwaves (Evans 2002) or millimeter waves (Fujii *et al.* 2007). The former technique has been integrated into a commercial termite detector called Termatrac™ (Evans 2002). However, the locomotion of beetle larvae is estimated to be slow, and such techniques are probably unsuitable for analysis of larval activities of *D. minutus*.

1.5. Objectives

The two techniques, X-ray CT and AE monitoring, were deemed promising for revealing the biology of *D. minutus* hidden with bamboo culms. Therefore, the objective of this research was to evaluate the applicability of these nondestructive techniques to analyze larval development and feeding behavior. Experiments designed for this purpose were conducted and are described in Chapters 2–4. The novelty and usefulness of these techniques and findings obtained by them are discussed from the viewpoint of entomology and pest management in Chapter 5.

Chapter 2. Evaluation of larval development and feeding behavior using X-ray computed tomography¹

2.1. Introduction

The life history and bamboo-attacking behavior of the bamboo powderpost beetle *Dinoderus minutus* are very difficult to investigate and, thus, remain poorly understood. The larval development and tunneling behavior are especially difficult to analyze because the larvae never leave bamboo culms before adult eclosion. X-ray computed tomography (CT) has proven to be an effective technique to nondestructively detect and analyze the presence and damage of insects in wood. As reviewed in Chapter 1, X-ray CT was used not only to observe insect tunnels and galleries but also to visualize the bodies of wood-boring insects (Bélangier *et al.* 2013, Fuchs *et al.* 2004, Himmi *et al.* 2014, Jennings and Austin 2011, Kigawa *et al.* 2009, Sone *et al.* 1995, Torigoe *et al.* 2010, Yanase *et al.* 2014). However, X-ray CT has never been used to visualize various stages of *D. minutus* inside bamboo culms or to trace the growth or behavior of any wood-inhabiting insects in the complete developmental periods.

In this chapter, the applicability of X-ray CT for evaluating the processes of larval growth and feeding, or tunneling, is discussed. First, in Section 2.2, artificially infested bamboo specimens were scanned using a microfocus X-ray CT system to evaluate the performance of the CT system for visualizing the beetles and tunnels and for tracing the growth and tunneling processes. Then, in Section 2.3, the same CT

¹ Section 2.2 originally published in: Watanabe, H., Yanase, Y., Fujii, Y. (2015a) Evaluation of larval growth process and bamboo consumption of the bamboo powder-post beetle *Dinoderus minutus* using X-ray computed tomography. *Journal of Wood Science* **61**(2), 171–177.

Section 2.3 originally published in: Watanabe, H., Yanase, Y., Fujii, Y. (2017a) Nondestructive evaluation of egg-to-adult development and feeding behavior of the bamboo powderpost beetle *Dinoderus minutus* using X-ray computed tomography. *Journal of Wood Science* **63**(5), 506–513.

system was used to trace and quantify the development and feeding from first instar to pupation and adult eclosion in bamboo pieces containing single individuals. Investigation from the first instar was facilitated by a method for egg collecting employing nutrient-containing filter paper. The feeding of newly eclosed pre-mating adults was also analyzed.

2.2. Visualization of larval growth process and tunneling process in infested bamboo culms

2.2.1. Materials and methods

Four bamboo pieces, 100 mm [longitudinal (L)] in length and approximately 35 mm [tangential (T)] in width, each with a node in the middle of its length, were prepared from partly moist culms of madake (*Phyllostachys bambusoides*) felled in May 2013 in Kyoto Prefecture, Japan. A laboratory strain of *D. minutus* reared on an artificial diet made of buckwheat flour (Suzuki and Kirton 1991) was used. A total of 25 adult beetles and the four bamboo pieces were enclosed together in a plastic container with a vent hole and were left undisturbed at room temperatures (25–29 °C) for two months to allow the beetles to reproduce. X-ray CT scans confirmed the existence of larvae inside the pieces.

One of the four bamboo pieces was used for CT scanning. This piece was split into three thinner specimens [approximately 12 mm (T) in width] so that their cross section would fit into the *xy* field of view when scanning (Fig. 2.1). All of the three split specimens were kept in a glass bottle with the fiber direction vertical and were scanned every 2–5 d (mostly every 3 d). During the two-month exposure, the specimens were considered to have reached an equilibrium moisture content (MC) of 12%, which was

obtained by oven drying of an uninfested bamboo piece under the same conditions.

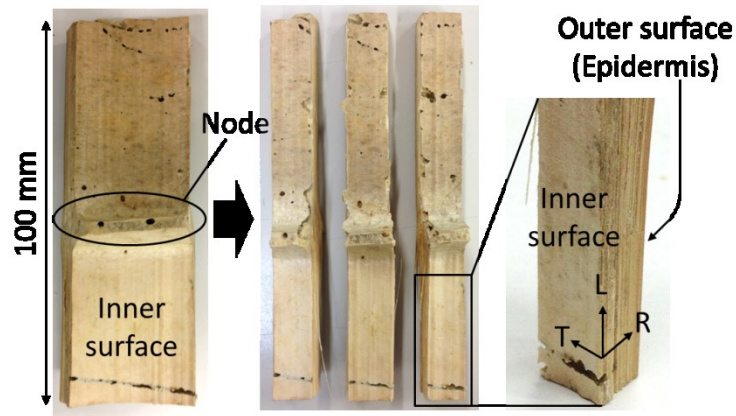


Fig. 2.1. Bamboo piece infested with *D. minutus*, split into three specimens. The holes and tunnels seen from outside were made by adult beetles.

Scans of the bamboo specimens were performed using a microfocus X-ray CT System (SMX-160CT-SV3S, Shimadzu Corp., Japan) with half-scan cone-beam CT (Fig. 2.2). “Microfocus” meant that the focal spot size of the X-ray tube was several micrometers, in the case of this system, 0.4 μm at minimum, resulting in high sharpness of high-resolution images. The X-ray source was operated with a tube voltage of 70 kV and a tube current of 80 μA . The volumetric data obtained from one scan consisted of 464 slices, each containing the cross-sectional image, or tomogram, of the scanned object in a dimension of 512×512 pixels. The voxel size and the slice pitch of the tomogram were both 61.9 μm under these scanning conditions, and the field of view was 31.7 mm along the x and y axes and 28.7 mm along the z axis. The scanning time was 320 s, during which time the scanned object was irradiated and rotated by approximately 180° . The specimens were set at a constant height for every scan, but the height was adjusted when a target larva had moved out of the z -axis field of view. The 3D volumetric data acquired from each CT scan was displayed in 2D grayscale images

of three orthogonal planes, which are referred to as “CT images”. In a CT image, the gray level of a pixel is an index of density; the brighter the pixel, the denser the area.

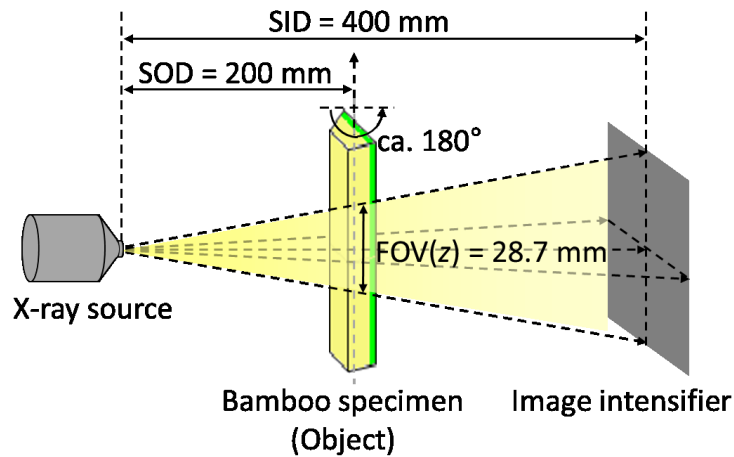


Fig. 2.2. Schematic diagram of the X-ray CT system. *SID* source to image intensifier distance, *SOD* source to object distance.

2.2.2. Results and discussion on larval growth and tunneling observed in CT images

The CT images provided a clear macroscopic view of the inside of the scanned bamboo specimens. Figure 2.3 shows example CT images capturing the silhouettes of the beetles. First, the bundle sheath fibers of the bamboo culm were separated from surrounding fundamental tissue composed of parenchyma cells, owing to the difference in density; the former were relatively brighter than the latter. Then, the silhouettes of insect bodies were apparent and had high gray value. The tunnels, whether they were hollow or filled with frass, were also visible, although in cases where the frass was as dense as the fundamental tissue of the specimens, the tunnels were not clearly separated. Furthermore, the stages of the beetle: larva, prepupa, pupa, and adult, were identified by the silhouettes.

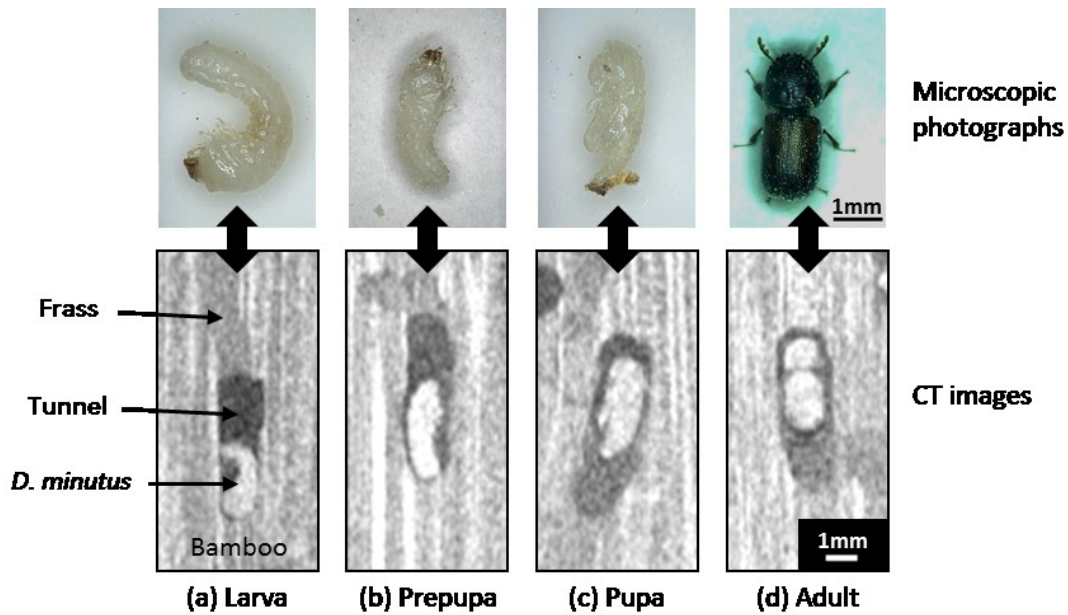


Fig. 2.3. Life stages of *D. minutus* captured in CT images (*below*), in comparison with microscopic photographs (*above*). The individuals shown in CT images are not the same as in the microscopic photographs.

In this experiment, a total of seven larvae were traced until pupation. Figure 2.4 shows an example of a series of CT images representing the movement of one of the larvae from the day it was first observed until it pupated. The larva was first observed on day 0 near the inner surface of the specimen. It bored downward along the fiber direction at all times. The entire tunnel was filled with dense frass, except for where the larva was present, until day 9. After day 13, a hollow part of the tunnel appeared, probably because the larva had bored a hole to the inner surface and frass was discharged from the hole. The larva seemed to have grown notably by day 13, but it was uncertain if the larvae had undergone ecdysis by then. On day 22, the silhouette of the larva is not seen clearly in the CT image, suggesting that it was not still during the 320 s of scan. The boring activity had stopped by day 22, and it was confirmed from the silhouette that the larva had pupated by day 25.

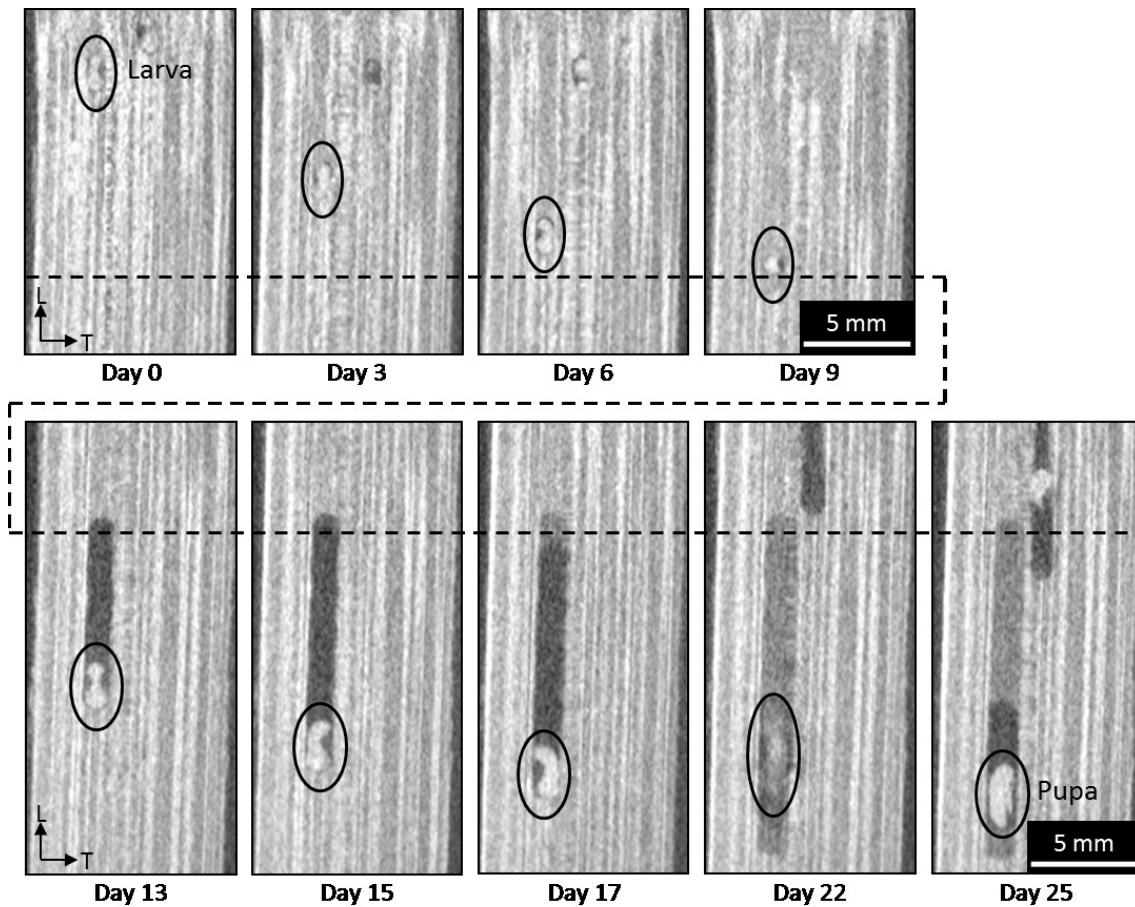


Fig. 2.4. CT images representing the tunneling process of a larva. *Dashed lines* indicate the same height.

Figure 2.5 shows the 3D elongation process of the tunnels of two larvae, larvae 1 and 2, in one specimen, which were first observed on the same day. Larva 1 is the same individual as shown in Fig. 2.4. The 3D image of the larval tunnels in Fig. 2.5 was created by marking only the pixels of the cross-section of the tunnels in each slice. Some parts of the tunnels where they are hollow were easily marked automatically by adjusting the threshold gray level using ImageJ 1.45s software (W. S. Rasband, National Institutes of Health, USA). However, it was difficult to automatically identify the parts of the tunnels where they were filled with dense frass, so they were marked manually. The 3D image was displayed using volume graphic software VGStudio MAX 2.0.5

(Volume Graphics GmbH, Germany). In contrast to the tunnel of larva 1, which was always bored linearly along the fibers, the tunnel bored by larva 2 was somewhat more complex. Larva 2 reversed its boring direction twice by day 13 and it bored slightly obliquely to the fiber direction between day 3 and day 9. The reason for this pattern of movement was not clear. Between day 17 and day 22, it bored in two different directions, probably to avoid encountering the nearby tunnel of larva 1.

The rest of the larvae exhibited similar movement patterns; they mostly bored along the fiber direction, but they sometimes reversed direction or bored obliquely to the fiber direction, possibly to avoid encountering other individuals or tunnels that could obstruct their movement. It was not possible to trace larvae when they were smaller than that shown in the first image of Fig. 2.4 because they were easily lost sight of in the CT images.

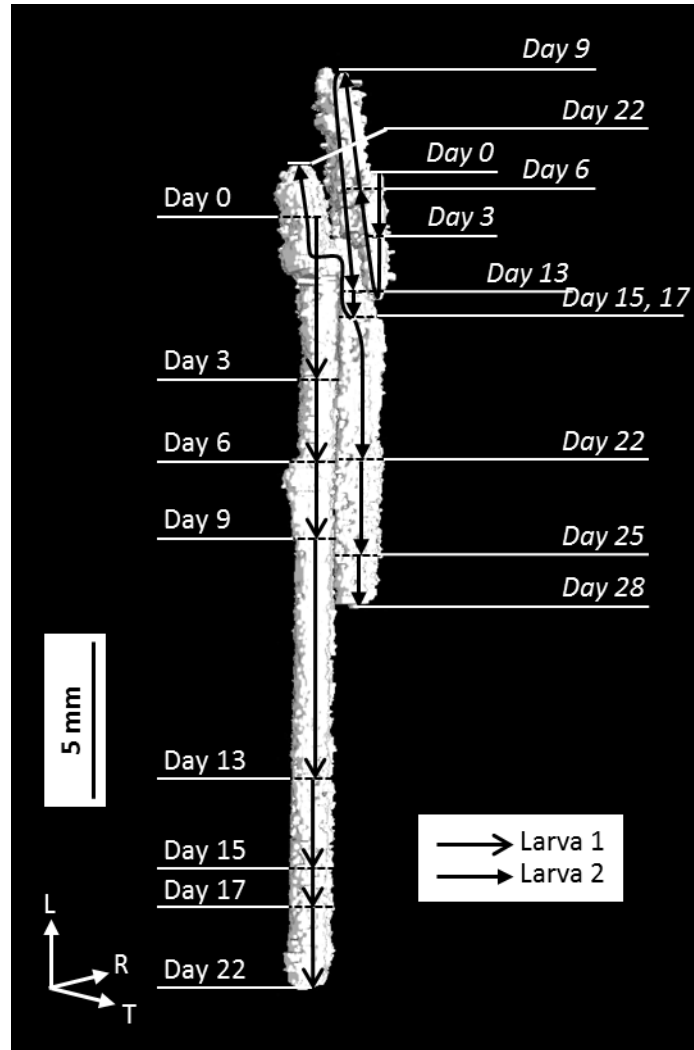


Fig. 2.5. 3D elongation process of the tunnels of larva 1 (*left*) and larva 2 (*right; labels italicized*) in the same specimen.

The obtained CT data seemed useful for quantitatively analyzing the process of tunneling and the bamboo consumption by the larvae. Possible methods were considered and described below. Changes in tunnel length could be easily measured in CT images. One method for calculating the volume of the tunnel was to accumulate the number of pixels in each slice that represented the cross section of the tunnel and convert it to a volume. However, it was often difficult to automatically identify the parts of the tunnel, as mentioned above, making this approach impractical. The tunnel volume

could be estimated by assuming that the cross section of the tunnel was elliptic and kept the same area in a scanning interval. The major and minor axes of the cross section of the tunnel (an example shown in Fig. 2.6) could be measured to calculate the cross-sectional area. The volume change from the previous scan could be estimated by multiplying the cross-sectional area by the increase in tunnel length. Images of the cross sections near the end of the tunnels were recommended to be used to measure the cross-sectional area because there was usually no frass around larvae at the end of the tunnels.

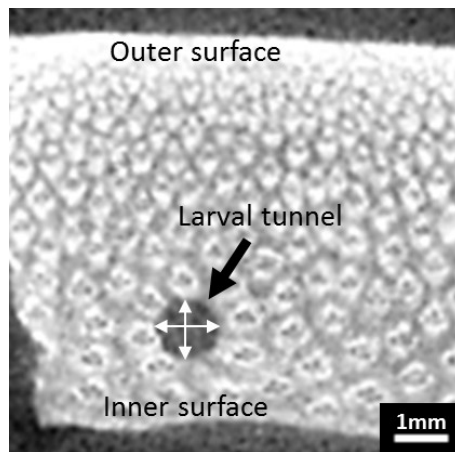


Fig. 2.6. Cross section of a larval tunnel. *White arrows* represent the two axes that could be used to calculate the cross-sectional area, assuming it to be elliptical.

So far, it was shown that the beetles in various developmental stages could be visualized and the process of larval tunneling was traceable using X-ray CT. Quantified larval growth and tunneling in the complete larval period will be discussed in the following section.

2.3. Evaluation of individual egg-to-adult development and feeding behavior

2.3.1. Egg collecting

Eggs of *D. minutus* are mainly deposited into bamboo metaxylem vessels (Garcia and Morrell 2009, Norhisham *et al.* 2015, Plank 1948, Ueda 1963, Wood Technological Association of Japan 1961). Collecting such eggs unharmed from bamboo pieces would be very difficult, and an alternative method was needed. Bletchly (1960) developed the “veneer technique” to collect eggs of the brown powderpost beetle *Lyctus brunneus*. Kartika and Yoshimura (2013) and Baba and Ainara (2014) reported more convenient techniques utilizing nutrient-containing filter paper to collect eggs of the powderpost beetle species *L. africanus* and *L. brunneus*, respectively. The latter techniques were adapted for *D. minutus*. Sheets of filter paper cut into 26 × 65 or 26 × 20 mm rectangles were soaked in an aqueous suspension containing 10% corn starch and 10% granulated sugar, and then dried at 60 °C for 1 h. Five-layered laminates of treated filter paper were formed by folding sheets of 26 × 65 mm four times or stacking five sheets of 26 × 20 mm. These laminates were fixed between two microscope slides with a string (Fig. 2.7). The laminates of filter paper were exposed to 10–20 adults of *D. minutus* inside Petri dishes and kept in an environmental chamber conditioned at 28 °C and 65% relative humidity (RH). Adults were obtained from laboratory strains reared on madake culms. The sexes of adults were not distinguished because adults do not have apparent morphological sexual characteristics (Abood *et al.* 2010). Many of the adults bored into the laminates of filter paper after exposure and, usually within 2 d, the females began to oviposit along the bored tunnels (Fig. 2.8a) or at the edges of the laminates. The boring behavior into laminates was not reported for *Lyctus* spp., which usually laid eggs at the edges (Baba and Ainara 2014, Kartika and Yoshimura 2013).

The eggs (Fig. 2.8b) were collected carefully using the tip of a writing brush, and the hatched larvae (Fig. 2.8c) were used for inoculation into bamboo pieces. Observations of 24 eggs showed that the average length and diameter were 0.84 ± 0.06 mm (mean \pm SD) and 0.15 ± 0.01 mm, respectively, the average incubation period was 5.0 ± 0.8 d, and the average body length of newly hatched first instar larvae was 0.79 ± 0.04 mm.

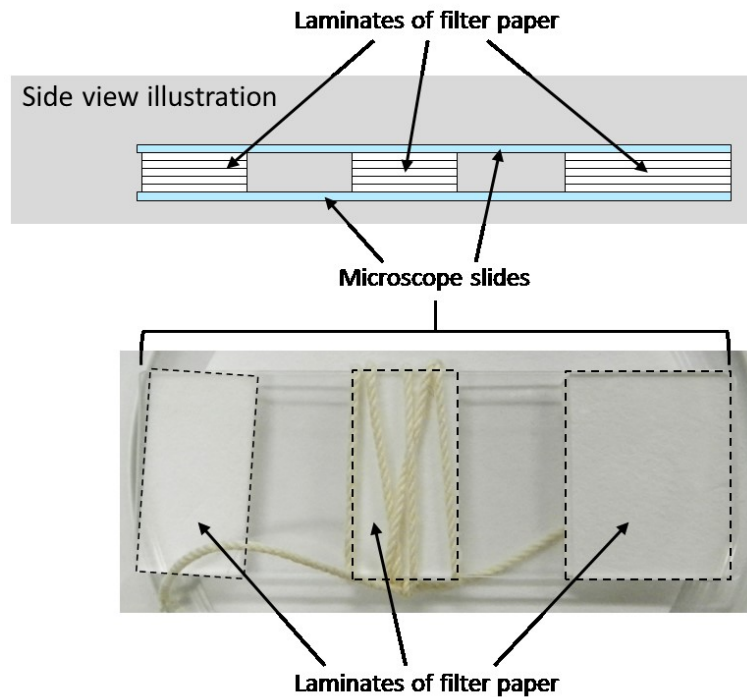


Fig. 2.7. Illustration and photograph of five-layer laminates of nutrient-containing filter paper, fixed between two microscope slides, used as oviposition sites of *D. minutus*.

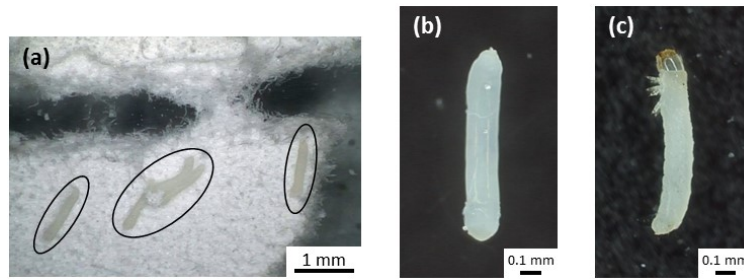


Fig. 2.8. Microscope photographs of eggs and a first instar larva collected from the laminates of filter paper. Note that photographs **a–c** do not show the same individuals. **a** Eggs (in *ovals*) laid between the layers of filter paper laminates along the tunnel bored by the adult beetle. **b** Egg removed from the filter paper. *Anterior end upper*. **c** First instar larva immediately after hatching. *Anterior end upper*.

2.3.2. Inoculation of larvae in bamboo and X-ray CT scanning

Air-dry internodes of madake culms [6–7 mm (R) thick] felled in June 2014 in Kyoto Prefecture, Japan, were split and cut into 14 pieces of 100 (L) × 20 (T) mm, which were used as the rearing medium. A hole with a depth of 5 mm was drilled longitudinally on one end surface of each piece with a 2.5-mm drill bit, and the hole was extended by 5 mm with a push pin (Fig. 2.9). The shape of this hole was recorded by CT scanning prior to inoculation. In addition, longitudinally aligned holes with a depth of 1.5 mm (R) and a diameter of 1.5 mm were drilled on the outer surface (epidermis) of each piece with intervals of 5–25 mm as location references (Fig. 2.9). A first instar larva immediately after hatching was randomly collected and placed in the hole on the end surface of each piece using a writing brush, and the hole was closed by inserting a round bamboo peg [3 mm (L) × \varnothing 2.5 mm]. The bamboo pieces were kept vertically, with the inoculated end surface on the top, in the environmental chamber

conditioned at 28 °C and 65% RH, in which the pieces were at 11% MC.

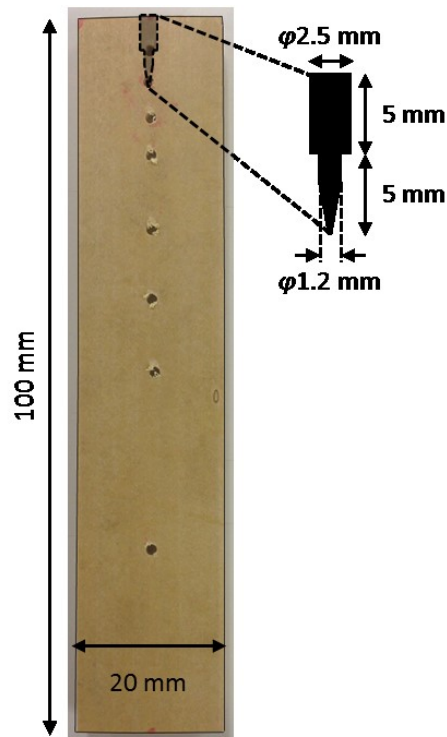


Fig. 2.9. Illustration of the bamboo piece with a hole for inoculation (not visible in the photograph) and aligned holes on the outer surface as location references.

The inoculated bamboo pieces were scanned using the same microfocus X-ray CT system every 3–5 d. Four different scanning protocols with different resolutions (voxel sizes) were employed according to the larval body size. The scanning parameters for each protocol are shown in Table 2.1. Protocol I, with the highest resolution, was used when the larval body length was approximately smaller than 1 mm, and later, protocols with lower resolutions and larger field of view were used to trace the larvae that tunneled for longer distances. Regardless of the employed protocols, the larval body lengths were mostly within 35–60 pixels and the axes of the tunnel cross sections were mostly within 15–25 pixels. The volumetric data obtained from one scan consisted

of 464–488 slices of 512×512 pixels. The scanning time during which the pieces were irradiated was 160 s. The distances from the X-ray source to the image intensifier and object were equal in Protocol IV and the scanning conditions employed in Section 2.2 (Fig. 2.2, Table 2.1), resulting in similar (but not exactly the same) resolutions. The average number in Protocols I–IV was halved from that employed in Section 2.2, resulting in reduction of time necessary for scanning and reconstruction.

Table 2.1. Scanning parameters for Protocols I–IV with different resolutions.

Protocol	I	II	III	IV
Tube voltage (kV)	60	60	65	70
Tube current (μA)	70	70	70	70
Source to image intensifier distance (mm)	400	400	400	400
Source to object distance (mm)	60	100	150	200
View number	600	600	600	600
Average number	16	16	16	16
Field of view (xy) (mm)	9.2–9.6	15	23	31
Field of view (z) (mm)	8.7	15	22	29
Voxel size and slice pitch (μm)	18–19	30	45	60

2D tomograms from the volumetric data were used to measure the larval body length, tunnel length, and tunnel cross-sectional area using ImageJ 1.47v software (W. S. Rasband, National Institutes of Health, USA). The larval body was curved except in the prepupal stage, so the body length was measured by the segmented line tool. The length of the tunnels was measured using the aligned holes on the outer surfaces as location references. The tunnel volume was estimated by assuming that the cross section of the tunnel was elliptic and kept the same area in a scanning interval of 3–5 d. The major and minor axes of the cross section of the tunnel near the end were measured to calculate the cross-sectional area. The volume change from the previous scan was estimated by

multiplying the cross-sectional area by the increase in tunnel length.

CT scans were continued after adult eclosion. The bamboo pieces containing adults were individually kept in glass bottles in the environmental chamber with no light source.

2.3.3. Results and discussion on larval–pupal development and larval feeding

Of the 14 first instar larvae, three either died or were lost track of by the time of the first CT scanning. The other 11 individuals all successfully pupated and emerged into adults. The results and discussion are based on these 11 individuals.

Figure 2.10 shows the growth and developmental process of a typical individual from first instar to adult captured in CT images. With the highest resolution (smallest voxel size) of 18 μm , silhouettes of the early stage larvae were visible in the CT images. The inoculated larvae tunneled into the parenchyma from near the tip of the inoculation holes made by the push pin. All of them bored downward, except one which bored upward at first but then reversed its direction after reaching the drilled part of the inoculation hole. The larvae bored linearly along the fibers most of the time. However, prior to pupation, three larvae created transverse tunnels in order to reach the surface and discharge frass from tiny holes; two larvae from the inner surface and one from the outer surface. This is the reason why, in Fig. 2.10, the tunnel was hollow after 66 d. Three other larvae bored slightly obliquely in the mature larval stages, one of which eventually reached the inner surface and discharged frass. Because the bamboo pieces were inoculated with single individuals, the larvae showed no complex tunneling patterns, as were observed in Section 2.2.

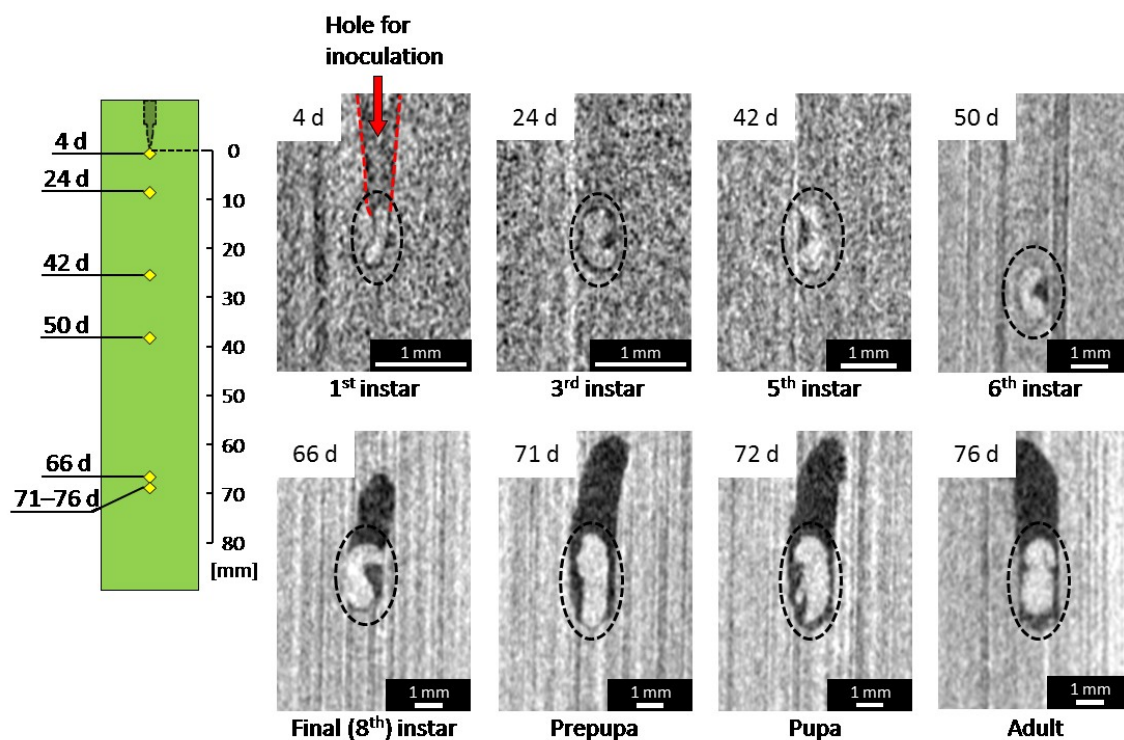


Fig. 2.10. Growth and development of an individual from first instar to adult captured in CT images. Scanning Protocol I was used for the *first* and *second* CT images on the *upper* row, Protocol II and III for the *third* and *fourth* images, respectively, on the *upper* row, and Protocol IV for the images in the *bottom* row. *Yellow squares* in the illustration of the bamboo piece on the *left* of the *figure* represent the approximate position of the beetle at the noted time elapsed after hatching. This individual is the same as the one named individual AX1 in Chapter 4. Larval instars given for reference were determined based on the result of AE monitoring in Chapter 4.

Figure 2.11 shows the time course of the body length of the 11 individuals from the first CT scan until adult eclosion. At first, the body lengths of all the larvae were smaller than 0.79 mm, the average body length of larvae immediately after hatching, suggesting that the larvae had shrunk. After the larvae had fully grown, they turned into prepupae and then pupated. However, the prepupal stage, lasting for approximately 1 d, was captured only for four larvae. The average body length in the final larval stage, including the prepupal stage if captured, was 3.53 ± 0.23 mm (mean \pm SD). The average

body lengths of pupae and adults were 3.42 ± 0.09 mm and 3.18 ± 0.17 mm, respectively. The average larval duration, calculated as the time from inoculation to the first observation of either the prepupal or pupal stage, was 61 ± 11 d. In this study, when discussing larval durations, the larvae were regarded as having pupated when the silhouettes of prepupae were captured. The total duration of larval and pupal stages, calculated as the time from inoculation to first observation of the adult stage, was 66 ± 11 d. The average pupal duration, therefore, was estimated to be 5 d. Although the larval growth was clearly observed, the CT images provided no clear evidence of ecdysis. This was because continuous analysis of growth or feeding was impracticable by CT scanning. As an alternative approach, the applicability of acoustic emission (AE) for continuous monitoring is discussed in Chapters 3 and 4.

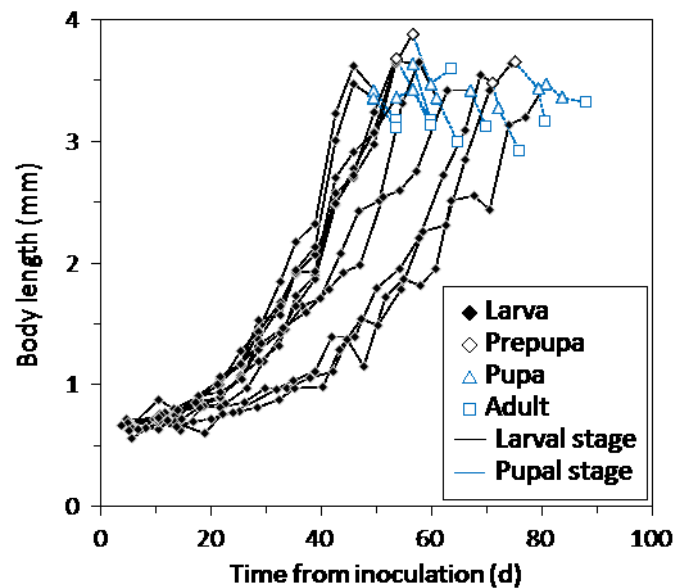


Fig. 2.11. Time course of body length of 11 individuals from the first CT scan to adult eclosion.

Figure 2.12 shows the time course of the tunnel length in the larval stage, until either the prepupal or pupal stage was first observed. Because the larvae filled their tunnels with frass as they extended their tunnels, the tunnel length represents the

distance they moved. The “tunneling speed” increased as the larvae developed from the first to final instars, and prior to pupation the tunnel length reached 80.2 ± 4.8 mm. The average tunneling speed for the entire larval stage was 1.34 ± 0.20 mm/d.

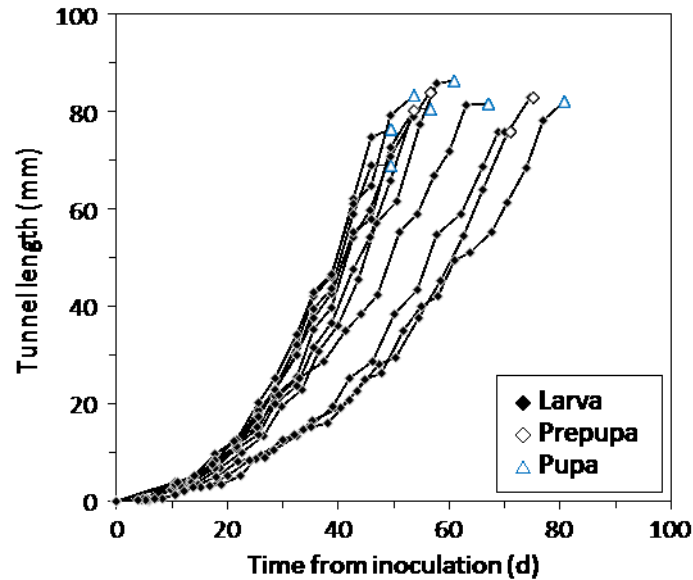


Fig. 2.12. Time course of larval tunnel length from inoculation to the prepupal or pupal stage.

Figure 2.13 shows the time course of the tunnel cross-sectional area, measured near the end of the tunnel where the area was largest, from the first CT scan to the prepupal or pupal stage. The cross-sectional area increased as the larvae grew and had a strong linear correlation with the square of the larval body length ($y = 0.145x^2 + 0.05$; $R = 0.98$). The final values of the cross-sectional area, 2.01 ± 0.13 mm² on average, represented the cross-sectional area of the pupal chambers, whose diameter was approximately 1.6 mm.

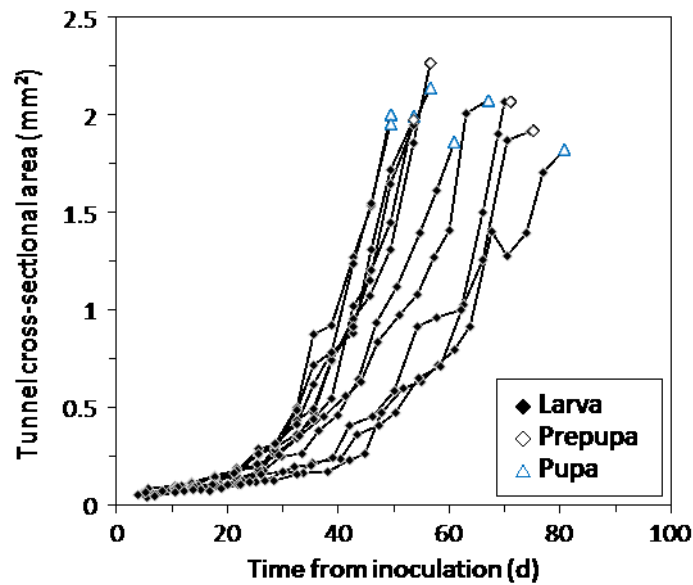


Fig. 2.13. Time course of larval tunnel cross-sectional area from the first CT scan to the prepupal or pupal stage.

Figure 2.14 shows the time course of the tunnel volume in the larval stage. The larvae bored and consumed $68.0 \pm 7.0 \text{ mm}^3$ of bamboo in the entire larval stage. At first, the volume consumed was small but it increased substantially as the larvae grew; the 90% of the total bamboo consumption was done in the latter 41% of the larval duration on average. This suggests that early detection and treatment can significantly reduce the extent of damage caused by the larvae. The correlations between total tunnel volume and final larval body length, pupal body length, and adult body length, respectively, were not especially high ($R = 0.46, 0.76,$ and, $0.43,$ respectively), and only the correlation between total tunnel volume and pupal body length was significant ($p < 0.01$). It is possible that parts of tunnels, for example, those made to discharge frass or made as pupal chambers, were not utilized as nutrient sources, causing variation in the tunnel volume and, hence, lower correlations.

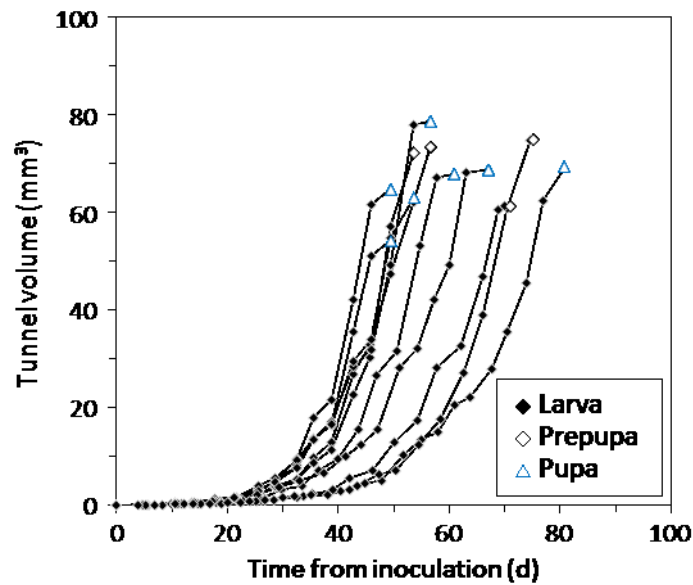


Fig. 2.14. Time course of larval tunnel volume from inoculation to the prepupal or pupal stage.

Using X-ray CT, larval attack of *D. minutus* was evaluated in terms of tunnel length and volume, which have not been reported previously for *D. minutus*, and this was a unique feature of utilizing nondestructive X-ray CT scanning. With the aid of laminated filter paper to collect eggs, the tunnel length and volume bored for the entire larval period per individual, as well as the time changes of these, were revealed for the first time. In addition, the growing body size and developmental period were measured without exposing or removing the larvae.

2.3.4. Discussion on larval duration

Irradiation, depending on the applied doses, can damage, sterilize, and kill living organisms and has been used to exterminate insects such as pests in fresh and stored foods (Follett 2004, Johnson and Marcotte 1999). Irradiated insect larvae may suffer delayed development and may fail to molt, pupate, or emerge into adults (Follett 2004, Johnson and Marcotte 1999). The irradiation doses at the surfaces of the bamboo

pieces or at the insect body surfaces during CT scans were not measured or estimated, but by comparing larval durations, the larval development was estimated to be unaffected by CT scanning. In Chapter 4, based on the results of AE monitoring of the larval development, it will be presented that the average larval duration of eight un-irradiated individuals was 64.8 d. The larval duration of irradiated larvae used for CT scanning was not significantly different from that of un-irradiated larvae ($p > 0.1$; Student's t -test). In addition, all of the successfully inoculated larvae pupated and emerged without abnormality after repeated CT scans. Therefore, the X-ray irradiation employed during CT scans was not considered to have hindered the development of the larvae.

Several previous reports from outside of Japan describe the larval duration of *D. minutus* and are summarized here for reference. Plank (1948) reported that, with monthly average temperatures of 26.0–26.8 °C, the larval duration was 41.4 ± 1.5 d (mean \pm SE, $n = 98$). Garcia and Morrell (2009) measured larval duration at different temperatures (15–30 °C) to determine the thermal thresholds and requirements, and at temperatures close to the experimental condition of this study: 25, 28, and 30 °C, the larval duration was 51.7 ± 1.2 d (mean \pm SE, $n = 24$), 46.3 ± 0.7 d (mean \pm SE, $n = 25$), and 43.8 ± 0.5 d (mean \pm SE, $n = 26$), respectively. According to Abood and Norhisham (2013) and Norhisham *et al.* (2015), the larval duration of individuals fed with cassava flour at 27 °C was 52.80 ± 0.31 d (mean \pm SE, $n = 50$) and that of individuals reared on bamboo at 25 °C was 44.2 ± 0.3 d (mean \pm SE, $n = 20$), respectively. The value of larval duration found in this study, 61 ± 3 d (mean \pm SE, $n = 11$), was longer than those reported previously, but these values cannot be simply compared because of underlying differences in many factors. As Garcia and Morrell (2009) showed, temperature greatly influences larval development. However, temperature hardly explains the differences

among these values because of the extremely low correlation ($R = 0.04$). Other possible factors may include regional and population differences and differences in species, nutrient contents, and moisture and other physical conditions of the employed rearing media. Some Japanese books describe the larval duration of *D. minutus* to be 20 d (The Society of House and Household Pests Science, Japan 1995) or 20–40 d (Tokyo National Research Institute for Cultural Properties 2001, Yamano 1976); however, the methods of examination are not noted in these books and the validity of these values cannot be discussed.

The larval duration varied greatly from 49 to 81 d in this experiment. The final larval body length, pupal body length, and adult body length were not significantly correlated with larval duration ($p > 0.1$). This suggests that, although the variation in larval duration, and hence the variation in rate of development, may be inherent in *D. minutus*, each larva is capable of developing into an adult of a certain body size. The variation in the developmental period may also explain the simultaneous presence of larval and adult stages throughout the year.

2.3.5. Pre-mating adult feeding

Adult beetles started boring new tunnels within 3 d after eclosion. They made holes that were smaller than their body size on the inner surfaces of bamboo and discharged frass from these holes. In 8 ± 1 d (mean \pm SD) after eclosion, they made exit holes on the inner surface, from which frass was also discharged. Even after making exit holes, the adults usually remained hidden inside the bamboo pieces. When the pupal chambers were not adjacent to the bamboo inner surface, the adults first bored obliquely to the fibers to reach the inner surface. Afterwards, most of the adults bored tunnels

parallel to the fibers, except two individuals whose tunnels were oblique to the fibers by 43° or 68°. An example CT image of a tunnel created in this period is shown in Fig. 2.15. The changes in tunnel length and volume bored by the adult beetles were measured in the same manner as those of the larval tunnels. Adults extended tunnels at average rates of 2.64 ± 0.58 mm/d in length and 4.87 ± 1.10 mm³/d in volume until they first made exit holes. The adult tunnels were slightly narrower than the pupal chambers, with an average cross-sectional area of 1.86 mm².

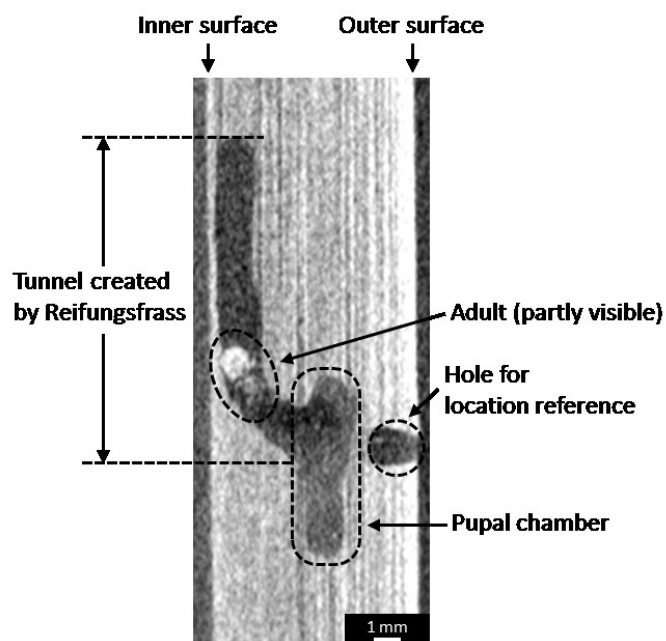


Fig. 2.15. CT image capturing a tunnel created by Reifungsfrass of the same individual as shown in Fig. 2.9, obtained at 8 d after adult eclosion.

The adult tunneling behavior described above corresponds to “Reifungsfrass”, a feeding behavior necessary for the maturation of newly emerged adults (Wood Technological Association of Japan 1961). The pattern of tunneling in the longitudinal direction during this period has been reported previously (Wood Technological Association of Japan 1961, Yamano 1976), and the result of this study, though with a few exceptions, was consistent with these reports. However, actual damage during

Reifungsfrass was quantified for the first time.

Mature adults exit the culms and mate, and mated females re-enter bamboo culms and bore new tunnels in which to lay eggs (Plank 1948, Ueda 1963, Wood Technological Association of Japan 1961, Yamano 1976). It was reported that female adults tunnel transversely to the bamboo fibers in the process of oviposition (Plank 1948, Wood Technological Association of Japan 1961, Yamano 1976). However, details of the extent of damage they cause during the ovipositional period are unknown, and nondestructive analysis of the ovipositional behavior is a topic of subsequent research.

2.4. Summary

In this chapter, two series of experiments were described. First, bamboo specimens artificially infested with *D. minutus* were scanned using a microfocus X-ray CT system every 2–5 days. Silhouettes of larvae, pupae, and adults were clearly recognizable in the CT images, and they were distinguishable from the bamboo, beetle tunnels, and frass. Then, individuals in separate bamboo pieces were traced from the first instar using the X-ray CT system with resolutions of 18–60 $\mu\text{m}/\text{voxel}$. Laminates of filter paper containing sugar and starch were an effective artificial oviposition medium and facilitated monitoring from the first instar. The collected eggs were 0.84 ± 0.06 mm (mean \pm SD) in length, and the egg duration lasted 5.0 ± 0.8 d. Based on CT images, the larvae grew to 3.53 ± 0.23 mm in body length and turned into pupae of 3.42 ± 0.09 mm. The larvae bored tunnels with a length of 80.2 ± 4.8 mm and a volume of 68.0 ± 7.0 mm³ over the larval period of 61 ± 11 d. CT scans were continued after adult eclosion to analyze pre-mating adult feeding. Newly emerged adults remained in the bamboo pieces to feed before making exit holes in 8 ± 1 d after adult eclosion. During this period, they

bored tunnels at rates of 2.64 ± 0.58 mm/d in length and 4.87 ± 1.10 mm³/d in volume. X-ray CT was an effective tool to nondestructively and quantitatively evaluate the development and feeding of *D. minutus*, and a methodology for the nondestructive evaluation of body size, tunneling behavior, and bamboo consumption in the egg-to-adult development was developed.

Chapter 3. Relationship between the movements of the mouthparts and the generation of acoustic emission²

3.1. Introduction

In the previous chapter, X-ray computed tomography (CT) was shown to be an effective tool to for nondestructively observing and quantifying the larval growth and tunneling of the bamboo powderpost beetle *Dinoderus minutus*. On the other hand, because of the inability to conduct continuous monitoring, uncertainty remained regarding the activity of the larvae between the CT scans. Acoustic emission (AE) drew the author's attention as an approach to monitor the feeding of larvae continuously. As reviewed in Chapter 1, AE monitoring has been applied as a nondestructive technique to detect invisible termite attack in wood and wooden constructions (Fujii *et al.* 1998, Yanase *et al.* 1999, 2001). Fujii *et al.* (1995) and Matsuoka *et al.* (1996) directly confirmed that AE waves were generated by the feeding activity of termites. AE monitoring was also applied to biological analyses of termite feeding under different conditions (Imamura and Fujii 1995, Indrayani *et al.* 2003, 2007a, 2007b). Furthermore, some studies dealt with AE detected from wood specimens inoculated with larvae of wood-boring beetles or wooden objects infested by beetles (Creemers 2013, 2015, Fujii *et al.* 1992, 1994, Imamura *et al.* 1998, Le Conte *et al.* 2015). These previous studies suggested that the feeding activity of *D. minutus* should generate AE events, and the detection of AE waves could allow continuous analysis of their feeding that was not accomplished by X-ray CT.

² Originally published in: Watanabe, H., Yanase, Y., Fujii, Y. (2016) Relationship between the movements of the mouthparts of the bamboo powder-post beetle *Dinoderus minutus* and the generation of acoustic emission. *Journal of Wood Science* 62(1), 85–92. The online publication of this article (doi: 10.1007/s10086-015-1525-4) contains electronic supplementary material, which is available to authorized users.

In order to evaluate the activity of *D. minutus* in bamboo culms by detecting AE waves from the bamboo surface, it is essential beforehand to confirm that the beetles' activities, most importantly feeding activity, actually produce detectable AE waves and to clarify the mechanism of AE generation. Although it was directly confirmed for four termite species that the feeding activity generated AE events (Fujii *et al.* 1995, Indrayani *et al.* 2007b, Matsuoka *et al.* 1996), no studies focused on the direct examination of AE events generated by coleopteran species. This chapter describes the experiment in which the behavior of *D. minutus*, both larvae and adults, on a small bamboo specimen was observed using a microscope camera while AE measurement of the bamboo specimen attached to an AE sensor was conducted simultaneously. The relationship between the movements of the mouthparts, particularly mandibles, of the larvae and adults and the generation of AE is discussed.

3.2. Materials and methods

3.2.1. Experimental insects and bamboo specimens

Bamboo specimens, 20 mm [longitudinal (L)] in length and 40 mm in arc length, were prepared from air-dry culms of madake (*Phyllostachys bambusoides*) felled in June 2014 in Kyoto Prefecture, Japan for the observation of larval feeding. The in-curved part near the inner surface of each specimen was shaped into a plane of 20 (L) × 28 [tangential (T)] mm with a laminate trimmer. A hole about the size of a larva was made with a drill bit and a chisel in the center of the trimmed plane of each specimen. A larva, which was taken from the artificial diet used for laboratory culture and was estimated to be in the final instar based on its head size, was placed in the hole of the specimen, and the hole was covered with a cover glass (Fig. 3.1).

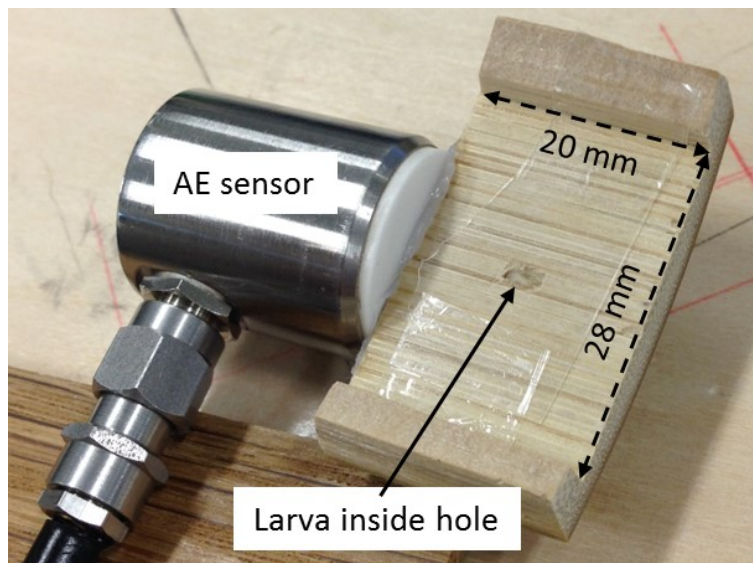


Fig. 3.1. Bamboo specimen for the observation of larval feeding, attached to the AE sensor.

Bamboo specimens with a different shape from the above-mentioned specimens were used for the observation of adult feeding. This was because an adult beetle would bore in the opposite direction to the microscope lens to avoid the light of the illuminator and it would be impossible to observe the mouthparts. The specimens, sheet-shaped with the dimension of 30 (L) × 10 (T) × 1.5 [radial (R)] mm, were prepared from the air-dry madake culms. A hole about the size of an adult was drilled through the center of the LT plane of each specimen with a bit. An adult, shortly after eclosion from pupa, was placed in this hole, and then the specimen was fixed between two microscope slides with binder clips (Fig. 3.2).

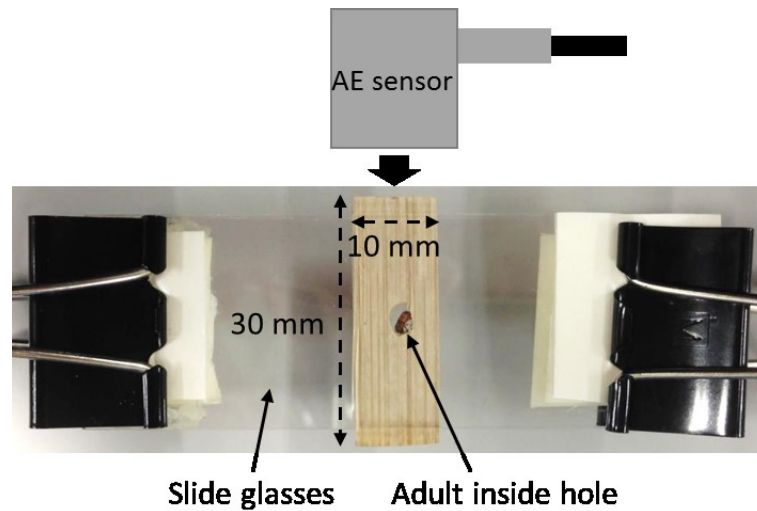


Fig. 3.2. Bamboo specimen for the observation of adult feeding.

3.2.2. Apparatuses

Some larvae and adults immediately began chewing the bamboo specimen after they were placed in it; others were left still for as long as overnight to wait for chewing behavior to be observed. When the larva or adult began chewing the specimen, a piezoelectric AE sensor (R15 α , Physical Acoustics Corp., USA) with a resonant frequency of 150 kHz was attached to the end surface of the specimen which was closer to the beetle's mouthparts than the other (Figs. 3.1, 3.2). A silicone grease was applied as an acoustic couplant between the specimen and the sensor. Because the sensor was insensitive to airborne noise, no sound-proof box was used in this experiment. The sensor was connected to a personal computer (PC) via an AE tester (AE9501A, NF Corp., Japan) and a PC-oscilloscope (DSO-2090 USB, Qingdao Hantek Electronic Co., Ltd., China). The AE signals from the sensor were amplified by 40 times and filtered by a high-pass filter with a cut-off frequency of 100 kHz. The signal waveform was acquired every time a trigger occurred and was displayed on the PC screen in real time,

as shown in Fig. 3.3. Because the trigger level was not constant, the threshold that defines an AE hit was later determined at 20.5 mV. Therefore, a signal that exceeded 20.5 mV in positive amplitude was counted as an AE hit. The amplitude display range was 398 mV, meaning that parts of the waveforms that exceeded this range would not be displayed or measured.

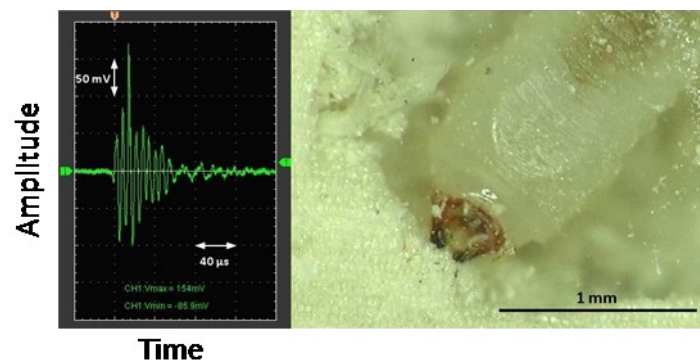


Fig. 3.3. Oscilloscope display where a signal waveform of burst emission is captured (*left*) and microscope image showing the mouthpart of a larva (*right*). Note that both the waveform and the microscope image have been cropped from the original display.

The larva or adult in the specimen was observed by the microscope (VH-5000, Keyence Corp., Japan), and the video images were displayed on the PC screen in real time with a resolution of 640×480 pixels, as shown in Fig. 3.3. The AE waveforms and video images were recorded by a screen capturing software (AG-desktop recorder Ver. 1.2.2, T. Ishii) with a frame rate of 16 fps. The experimental set-up is summarized in Fig. 3.4. The experiment was conducted in the laboratory at a temperature of 25 °C. Four different individual larvae and three different individual adults were used for observation and analysis.

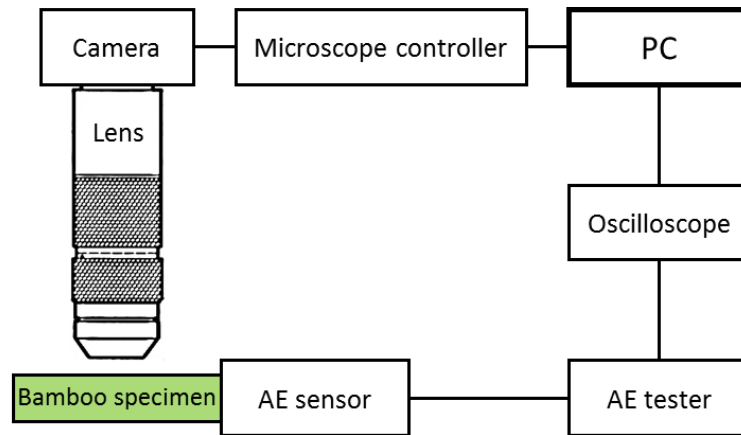


Fig. 3.4. Schematic diagram of the experimental system.

A control specimen with no beetle was also used for AE measurement to examine the presence of noise signals. The number of AE hits detected from the control specimen within 150 s of measurement was 0–3, suggesting that the noise signals would hardly affect the results of the experiment.

3.2.3. Measurement of time lags between AE signals and video signals

Possible time lags between AE signals and video signals displayed on the PC screen in this experimental system were measured using the pencil lead break as a simulated AE source. The method of the pencil lead break was based on NDIS 2110 (1997). A bamboo specimen [10 mm (L) in length and 40 mm in arc length] was prepared from the air-dry madake culm. The AE sensor was fixed so that the detection face would face up, and the specimen was vertically placed on the detection face with the silicone grease couplant. The pencil lead break was performed six times on the end surface of the specimen, and this process was filmed by the microscope camera, with the lens fixed horizontally. On the PC screen, AE signal waveforms and video images were displayed and captured. As a result, the first frame capturing the broken lead

appeared 1–2 frames (1.5 frames on average) after the first frame capturing the waveform originating from the pencil lead break appeared. Therefore, when an AE waveform was detected in a frame of the recorded video clips of *D. minutus* feeding, the next frame or the frame after next was assumed to show the microscope image of the moment of AE generation.

3.2.4. Analysis

The behavior of the larvae and adults was separated into “chewing” and “non-chewing”. When the beetle applied its open mandibles to the bamboo specimen, brought them together medially, and reopened them, such movement of the mandibles was defined as a “chewing movement”. Any movement of the mandibles in which the mandibles never touched the specimen was not regarded as a chewing movement. Parts of the video clips in which the mandibles were unclearly observed were not used for analysis. Figure 3.5 shows the relationship between the number of AE hits detected in the “chewing phases” observed in a video clip and the length of the chewing phases. The number of the chewing movements of the mandibles in each video clip was counted by visual observation, and the detection of AE hit(s) was examined in each chewing movement. To support the results of the observation, example video clips (ESM 1–4) were prepared as electronic supplementary materials. The ESM video clips are appended to the online publication of the original article (doi: 10.1007/s10086-015-1525-4).

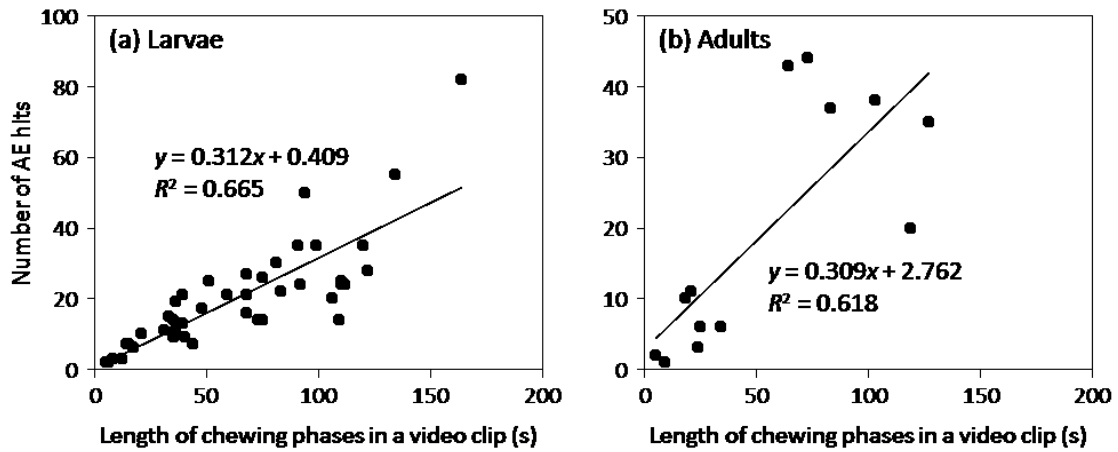


Fig. 3.5. Relationship between the number of AE hits detected in the chewing phases observed in each video clip and the length of the chewing phases. Different individuals are not distinguished in this figure.

3.3. Results and discussion

3.3.1. Larval feeding

In the “chewing phases”, the larval mandibles were almost constantly in chewing movements. Table 3.1 shows the number of chewing movements of the mandibles and the number of AE hits detected in the chewing phases of the four larvae. The number of chewing movements observed in the total analysis time T (s) is indicated by n in Table 3.1. There were two types of chewing movements: those in which one or more AE hits were detected and those in which no AE hits were detected. The former is referred to as “AE-generating chewing movements” and the number of them is indicated by m . The total number of AE hits detected in T is indicated by a .

Table 3.1. Relation between the number of chewing movements of mandibles and AE hits detected in the chewing phases of the larvae.

Larva	Number of chewing movements n	Number of AE-generating chewing movements m	Ratio of AE-generating chewing movements m/n	Number of AE hits generated in chewing movements a	AE hits per AE-generating chewing movement a/m	Total analysis time T (s)	Chewing movements per second n/T
I	1229	316	0.26	349	1.1	1461	0.84
II	593	212	0.36	268	1.3	646	0.92
III	180	76	0.42	88	1.2	219	0.82
IV	292	117	0.40	148	1.3	352	0.83

Signals of burst AE were detected in the AE-generating chewing movements of the mandibles, as shown in the video clip of larva I (ESM 1), and the number of detected AE hits in the chewing phases was significantly larger than the possible number of noise signals. The AE waveforms contained the principal frequency component corresponding to the resonant frequency of the sensor, 150 kHz, although a wide range of frequencies was estimated to be produced. Figure 3.6 shows an example series of successive frames of the video clip (ESM 1) capturing the moment of AE detection and a chewing movement of the mandibles. The mandibles of the larva gradually came together from the first frame (Fig. 3.6a) to the sixth frame (Fig. 3.6f). A newly detected AE waveform appears in the third frame (Fig. 3.6c). Since the video signals were delayed from the AE signals by 1–2 frames, the mandibles are estimated to have triggered the AE event in the fourth frame (Fig. 3.6d) or fifth frame (Fig. 3.6e).

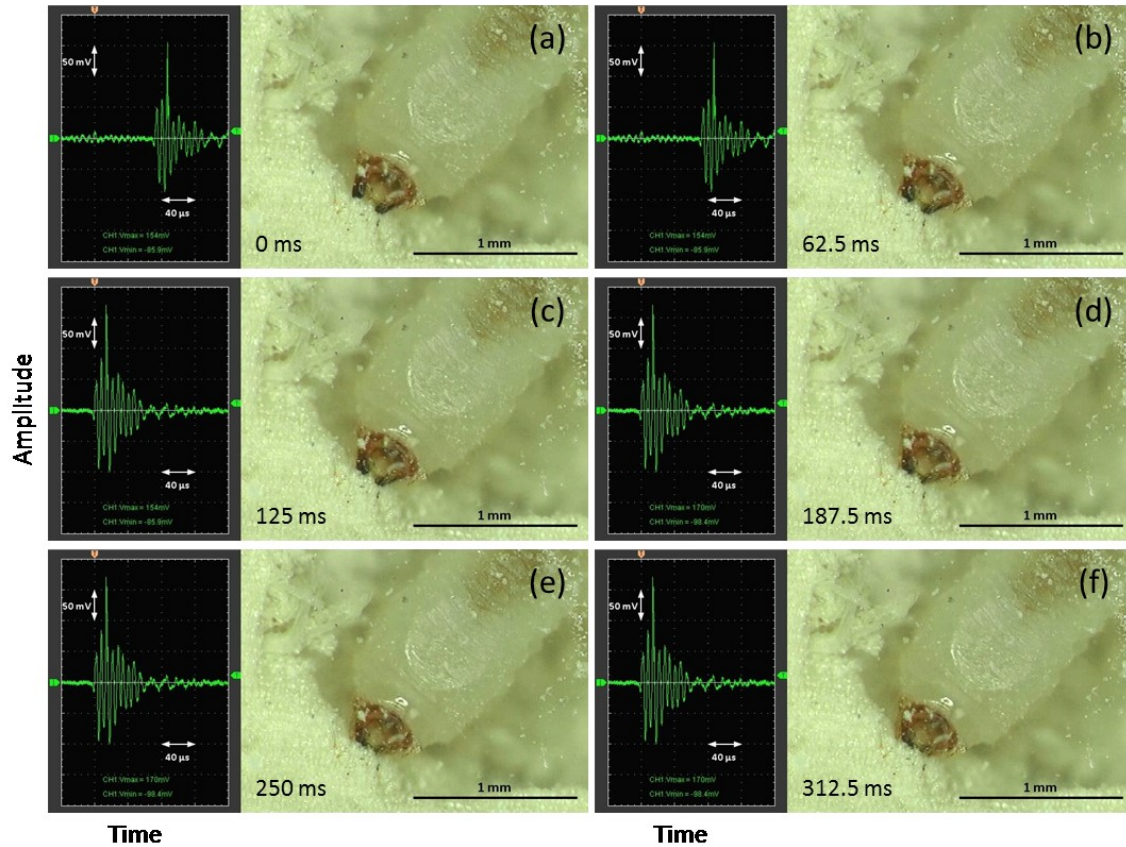


Fig. 3.6. Series of frames of the video clip (ESM 1) capturing the moment of AE detection and a chewing movement of the mandibles of larva I. Each frame consists of the waveform of the AE signal (*left*) and the microscope image of the larva (*right*). Note that both the waveforms and the microscope images in the video clip have been cropped from the original video.

Table 3.1 and ESM 1 also show that AE hits were not always detected in every chewing movement. The ratio of AE-generating chewing movements m/n was smaller than 0.5 for any larva (Table 3.1), implying that the majority of chewing movements did not produce detectable AE hits. However, all AE hits were detected when the mandibles were in chewing movements, suggesting that AE waves were generated by the chewing movements of the mandibles. When no AE hit was detected in a chewing movement, the chewing movement may have produced AE signals that did not exceed the threshold level. Additionally, the possibility cannot be denied that a movement in which the mandibles never touched the specimen was regarded as a chewing movement.

One AE-generating chewing movement usually produced one AE hit. However, the ratio of detected AE hits to the number of AE-generating chewing movements a/m is greater than 1 (Table 3.1). This is because more than one hit was detected in some of the chewing movements, as shown in the distribution of the number of AE hits detected in one AE-generating chewing movement of larva I (Fig. 3.7). As an example, a chewing movement in which three AE hits were detected is observed at around 15 s of the video clip (ESM 1). In some cases, the later AE wave had smaller amplitude than the earlier wave, and the later wave seemed like the reflection components of the earlier wave. However, the velocities of AE waves propagating longitudinally in madake culms measured preliminarily suggested that the reflection components would appear in the same frame as the original wave under the measurement conditions employed. Therefore, when more than one AE hit was detected in a chewing movement, the movement produced more than one AE event. The reasons for this were considered, but were not clarified.

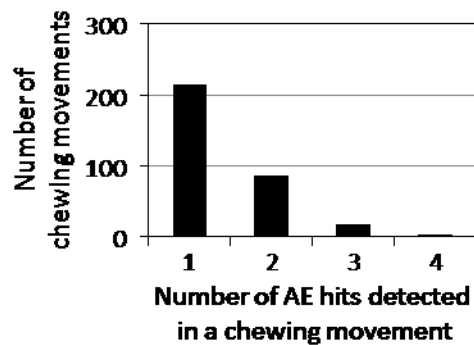


Fig. 3.7. Distribution of the number of AE hits detected in one chewing movement of larva I.

An example video clip of the “non-chewing phase” of larva I is shown in ESM 2. In this video clip, although the larval body was moving, no chewing movements of the larval mandibles were observed, and no AE hits were detected. Table 3.2 shows the

lengths of the non-chewing phases and the number of AE hits detected in these phases. Only one hit was detected in the analyzed non-chewing phases. This concluded that almost all AE hits detected in the chewing phases were produced by the chewing movements of the mandibles.

Table 3.2. Number of AE hits detected in the non-chewing phases of the larvae.

Larva	Total analysis time (s)	Number of AE hits
I	181	1
II	93	0
III	141	0
IV	150	0

Figure 3.8 shows the distribution of the peak-to-peak (P-P) amplitude of the AE hits detected in the chewing phases of larva I. The P-P amplitude values of detected AE hits varied greatly, and on average, 21% of the hits detected from all larvae had P-P amplitude values that were larger than the display range of 398 mV. It is reported that the amplitude values of AE waves produced by termite species differed among the types of feeding behavior and “pulling” behavior produced largest amplitude (Indrayani *et al.* 2007b, Matsuoka *et al.* 1996). However, in this experiment, no specific pattern of chewing movements was observed in the behavior of *D. minutus* larvae when the P-P amplitude values of AE hits were relatively large. The amplitude may have depended on the types of bamboo tissue, with different physical or mechanical properties, that were being bitten at or off by the larva. The occurrence of AE waves that have large amplitude is crucial in the practical application of AE detection because AE waves with smaller amplitude would not be detected owing to the attenuation in the long bamboo

culms.

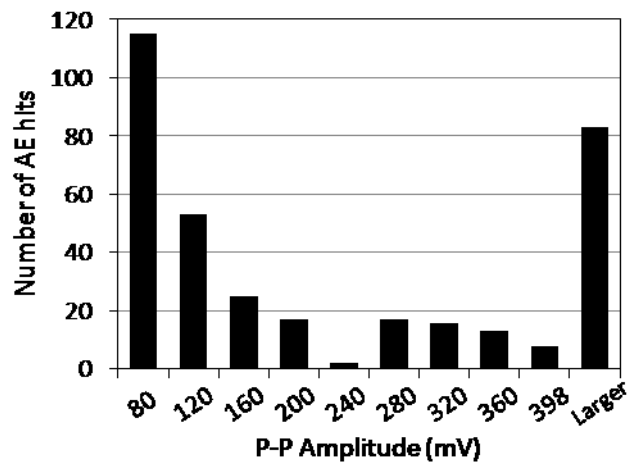


Fig. 3.8. P-P amplitude distribution of AE hits detected in the chewing phases of larva I.

It was difficult to observe the fragments that were bitten off by the larvae. However, larva II actually consumed a part of the specimen near its head, and particles of excreta were produced near its abdomen within 4 h (Fig. 3.9). This suggested that the chewing behavior discussed thus far was certainly feeding behavior. This also suggested that larval frass of *D. minutus* consisted mostly of excrement. It should be noted that, in contrast to workers or pseudergates of termites which can pull wood fragments off with the aid of their legs as props (Indrayani *et al.* 2007b), the short larval legs of *D. minutus* appear to have no such function. Although the observed larvae sometimes seemed to be pulling bamboo fragments after they brought the mandibles together by slightly withdrawing the head, the removal of bamboo fragments was estimated to rely mostly on the to-and-fro chewing movements of the mandibles.

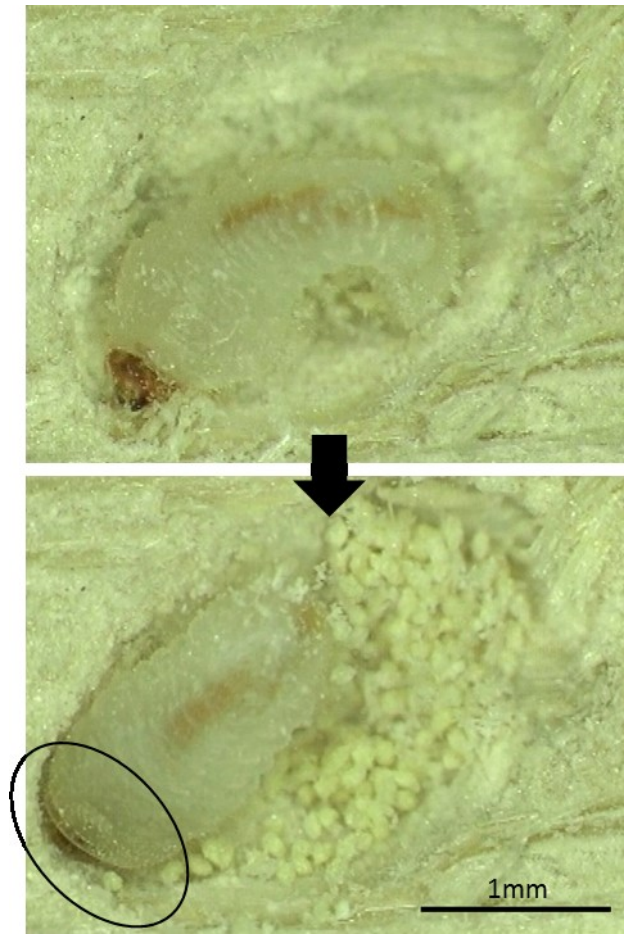


Fig. 3.9. Part of the bamboo specimen marked with an *oval* was consumed by larva II and particles of larval excreta were produced within 4 h.

From the above results, it was directly confirmed that the feeding behavior of the larvae triggered the generation of AE events. Therefore, AE monitoring can be applied to the continuous analysis of the feeding of *D. minutus* larvae.

3.3.2. Adult feeding

An example video clip of the chewing phase of adult I is shown in ESM 3. Figure 3.10 shows an example frame of the video clip (ESM 3). The adults had larger mandibles than the larvae. The movements of adult mandibles were similar to those of the larvae, and the video clips were analyzed in the same manner. Table 3.3 shows the number of chewing movements of the mandibles and the number of AE hits detected in the chewing phases of the three adults. AE hits were detected in the chewing phases as the adult chewed the specimen with its mandibles. As in larval chewing movements, AE hits were not always detected in every chewing movement, and the ratio of AE-generating chewing movements to all chewing movements m/n was 27–43% (Table 3.3). However, all AE hits were detected when the mandibles were in chewing movements. One AE-generating chewing movement usually produced one AE hit, but the ratio of detected AE hits to the number of AE-generating chewing movements a/m is greater than 1 (Table 3.3) because more than one hit was detected in some of the chewing movements. The frequency of chewing movements, represented as n/T , was similar between the larvae (Table 3.1) and adults (Table 3.3). On average, 19% of the AE hits detected from the adults had P-P amplitude values larger than 398 mV, which was also similar to the case of the larvae. However, the adults with larger mandibles may be able to produce AE waves with larger amplitude than the larvae, although it was unclear from this study.

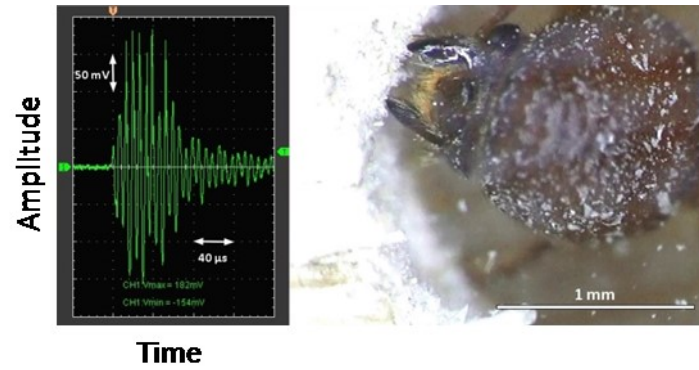


Fig. 3.10. Frame of the video clip (ESM 3) of adult I. *Left* waveform of the AE signal, *right* microscope image. Note that both the waveforms and the microscope images in the video clip have been cropped from the original video.

Table 3.3. Relation between the number of chewing movements of mandibles and AE hits detected in the chewing phases of the adults.

Adult	Number of chewing movements n	Number of AE-generating chewing movement m	Ratio of AE-generating chewing movements m/n	Number of AE hits generated in chewing movements a	AE hits per AE-generating chewing movement a/m	Total analysis time T (s)	Chewing movements per second n/T
I	243	86	0.35	101	1.2	233	1.0
II	171	73	0.43	83	1.1	171	1.0
III	243	66	0.27	74	1.1	306	0.79

Table 3.4 shows the lengths of the non-chewing phases and the number of AE hits detected in these phases. An example video clip of the non-chewing phase of adult I is shown in ESM 4. No AE hits were detected in the non-chewing phases. Therefore, AE hits detected from the specimens in the chewing phases were produced by the chewing movements of the mandibles of the adults.

Table 3.4. Number of AE hits detected in the non-chewing phases of the adults.

Adult	Total analysis time (s)	Number of AE hits
I	36	0
II	28	0
III	131	0

3.4. Summary

In the study described in this chapter, the observation of the mandible movements of *D. minutus* in the bamboo specimen and AE measurement of the specimen were conducted simultaneously, in real time. Practically all AE waves were detected when the larvae or adults were chewing the specimens, confirming that the chewing movements of the mandibles triggered the generation of AE events. This result suggests that the detection of AE waves reflects the feeding of *D. minutus*. Therefore, this study supports the potential of AE monitoring as a nondestructive tool to evaluate the feeding of this beetle.

Chapter 4. Combined use of acoustic emission and X-ray computed tomography to monitor larval feeding activity and development³

4.1. Introduction

In Chapter 2, X-ray computed tomography (CT) was shown to be an effective tool for nondestructively observing and quantifying the larval growth and tunneling of the bamboo powderpost beetle *Dinoderus minutus*. On the other hand, because of the inability to conduct continuous monitoring, uncertainty remained regarding the activity of the larvae between the CT scans. Therefore, in Chapter 3, it was demonstrated directly that the chewing movements of the mandibles of *D. minutus* in feeding produced acoustic emission (AE) waves, and the effectiveness of AE monitoring for continuous analysis of their feeding activity was proposed. In addition, a preliminary experiment suggested that periods of ecdysis and pupation could be estimated using AE monitoring (Watanabe *et al.* 2015b). It was, therefore, suggested that combined use of AE monitoring and X-ray CT could comprehensively clarify the relationships among the transitions of feeding activity, larval development, and the amount of bamboo consumed by the larvae.

This chapter describes AE monitoring of the feeding activity of *D. minutus* inside bamboo pieces conducted continuously from the first instar to adult eclosion. The obtained data were used to nondestructively determine the number of ecdysis events and the time period of each instar and to discuss the rhythmic patterns of feeding activity. X-ray CT scanning was used for selected individuals to relate the AE data to the

³ Originally published online in: Watanabe, H., Yanase, Y., Fujii, Y. (2017b) Continuous nondestructive monitoring of larval feeding activity and development of the bamboo powderpost beetle *Dinoderus minutus* using acoustic emission. *Journal of Wood Science* doi: 10.1007/s10086-017-1678-4, 11 pp.

developmental stages and bamboo consumption. Several additional experiments were conducted to directly observe the process of ecdysis, to estimate larval head capsule widths of all instars, and to discuss the effects of attenuation of AE waves on the AE monitoring of feeding activity. AE monitoring was continued after adult eclosion to analyze the pre-mating feeding activity of adult beetles.

4.2. Materials and methods

4.2.1. Preparation of bamboo pieces and inoculation of larvae

Bamboo pieces, 100 [longitudinal (L)] × 20 [tangential (T)] mm, were prepared from air-dry internodes of madake (*Phyllostachys bambusoides*) culms, 6–7 mm [radial (R)] thick, felled in June 2014 in Kyoto Prefecture, Japan. Eggs of laboratory strains of *D. minutus* reared on madake culms were collected using laminates of nutrient-containing filter paper, as described in Chapter 2, and newly hatched first instar larvae were collected randomly for inoculation into the bamboo pieces. A hole with a depth of 5 mm was drilled longitudinally on one end surface of each bamboo piece with a 2.5-mm drill bit, and the hole was extended by 5 mm with a push pin. A newly hatched larva was placed individually into this hole, and the hole was closed using a round bamboo peg. Then, a piezoelectric AE sensor (R15α, Physical Acoustics Corp., USA) was glued onto the same end surface as where inoculation was performed with a cyanoacrylate adhesive (Fig. 4.1). After 2 h, the pieces were placed vertically, with the inoculated end surface on top, in an environmental chamber, and AE measurement was started. The environmental chamber was conditioned at 28 °C and 65% relative humidity, where the moisture content (MC) of the bamboo culms was 11%. No light source was employed throughout the experiment. Also, because the sensors were

insensitive to airborne noise, no soundproofing measures were employed.

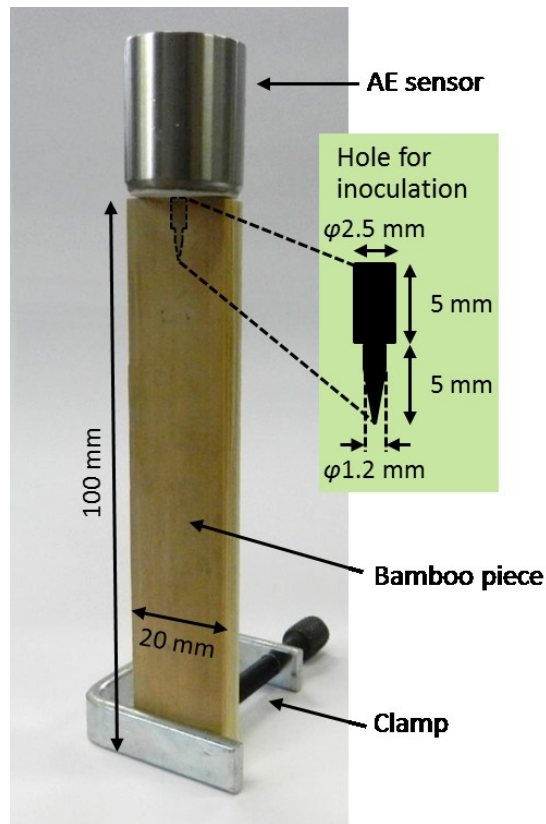


Fig. 4.1. Illustration of the bamboo piece with a first instar larva inoculated in the hole and an AE sensor glued onto the upper end surface.

To obtain ten replicates, 17 inoculated pieces were prepared. Of the 17 first instar larvae, 11 individuals successfully started feeding, but one individual ceased feeding after the first instar, suggesting that it had died in the process of ecdysis. The results and discussion are based on the surviving ten individuals.

Of these ten individuals, randomly chosen two individuals, AX1 and AX2, were also subjected to CT scanning using a microfocus X-ray CT system (SMX-160CT-SV3S, Shimadzu Corp., Japan), usually with an interval of 3–5 d. Scans were performed daily when pupation and adult eclosion approached. These two individuals were included in the 11 individuals used for CT scanning in Section 2.3 of

Chapter 2. It is advised to refer to Chapter 2 for methods of CT scanning and measurement of larval tunnel length and volume. The eight individuals that were not used for CT scanning are referred to as A1–A8.

4.2.2. AE measurement and analysis

AE data were acquired using a 4-channel AE system (DiSP with AEwin, Physical Acoustics Corp., USA). Each of the AE sensors, with a resonant frequency of 150 kHz, was connected to the system via a preamplifier (1220A, Physical Acoustics Corp., USA), as outlined in Fig. 4.2. The AE signals detected by the sensor were filtered by a 100–400 kHz bandpass filter and amplified by 40 dB in the preamplifier and by 20 dB in the system amplifier. The signals were then discriminated at a threshold of 80 dB, and a burst signal that exceeded this threshold in positive or negative amplitude was counted as an AE hit. It should be noted that the definition of a hit is slightly different from that in Chapter 3 because a different measurement system was employed. The time of detection and amplitude, i.e., the maximum (positive or negative) signal excursion during the hit, were recorded for each hit. The AE hits were determined using the hit definition time (HDT) of 100 μ s, the hit lockout time (HLT) of 200 μ s, and the peak definition time (PDT) of 40 μ s. The amplitude values of AE hits were expressed in dB with a reference voltage of 1 μ V.

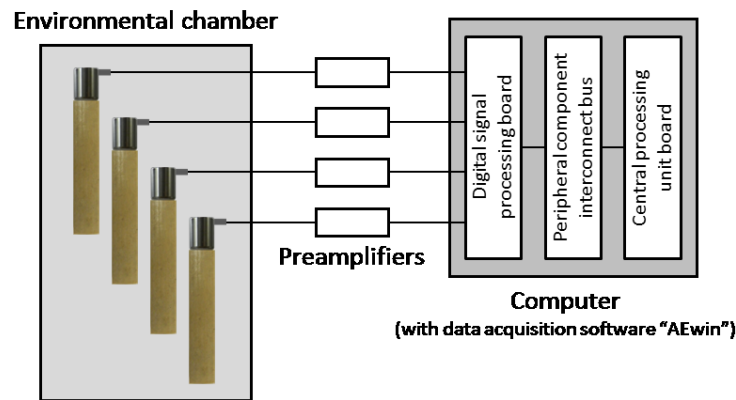


Fig. 4.2. Schematic diagram of AE measurement system for bamboo pieces containing *D. minutus* larvae.

Two parameters were defined to express the AE data in this experiment: hourly AE hit rate and mean maximum amplitude. Hourly AE hit rate was the number of AE hits detected in 1 h, and mean maximum amplitude was calculated as the hourly mean of six maximum amplitude values recorded during 10-min intervals. In addition, frequency spectra of the time courses of the number of AE hits per 5 min calculated using fast Fourier transformation (FFT) were used to analyze the periodicity of larval feeding activity found in this experiment.

After adult eclosion, bamboo pieces containing adults were kept separately in glass bottles, and AE measurement was continued. The threshold was raised to 85 dB prior to adult eclosion.

4.2.3. Direct observation of ecdysis and pupation (Additional experiment I)

In order to verify that the larvae underwent ecdysis or pupated during periods of no AE detection, additional larvae were inoculated in bamboo pieces by placing inside holes made with a 1.5-mm drill bit and the pieces were subjected to AE monitoring. When AE detection from these pieces stopped, the larvae were extracted

and the process of ecdysis was observed using a microscope (VH-5000, Keyence Corp., Japan). A microscope image of the larva was recorded every 300 s in the environmental chamber. Two first instar larvae and five larvae in middle or later instars were used for observation.

4.2.4. Measurement of distance attenuation of elastic waves in bamboo (Additional experiment II)

The amplitude attenuation of longitudinally propagating elastic waves per unit distance was measured by inputting continuous waves into bamboo culms of different lengths. Three bamboo specimens [300 (L) × 20 (T) mm] were prepared from air-dry internodes of madake culms [6–7 mm (R) thick] at 8–9% MC and with an air-dry density of 0.87–0.89 g/cm³. Elastic waves were input from one end surface of each specimen, and the amplitude of the waves was measured at the other end surface. Then, the length of the specimen was shortened by 50 mm and the same procedure was repeated four times, until the specimen's remaining length was 100 mm. The input signals of continuous sinusoidal waves with a frequency of 150 kHz were generated using a digital function generator (DF1906, NF Corp., Japan) and were transduced and transmitted through a piezoelectric actuator (the same model as the AE sensors). In order to simulate AE waves generated by *D. minutus* larvae, a push pin was inserted into the end surface of the specimen, 2 mm below the inner surface, and the transmitter was fixed to the head of the push pin. A receiver AE sensor was attached to the other end surface of the specimen, and output signals detected by the receiver were acquired using an AE tester (AE9501A, NF Corp., Japan). A silicone grease was applied as an acoustic couplant between the transmitter and the push pin, and between the specimen and the receiver. The transmitter, the specimen, and the receiver were held together with a

clamp. The amplitude of the output signals was displayed using a PC-oscilloscope (DSO-2090 USB, Qingdao Hantek Electronic Co., Ltd., China). The measurement system is summarized in Fig. 4.3. The attenuation in dB/mm was calculated as the slope of the regression line relating the amplitude level of the output signals to the propagation distance (length of the specimen).

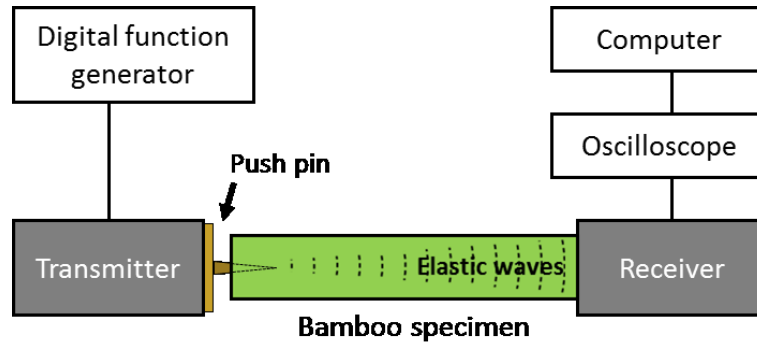


Fig. 4.3. Schematic diagram of the measurement system for attenuation of elastic waves in bamboo culms.

4.2.5. Measurement of amplitude of AE generated by larvae of different instars (Additional experiment III)

In order to discuss the relationship of AE amplitude to larval head size and instars, AE signals generated by larvae of various body sizes were recorded, with the propagation distances kept constant. Four newly hatched first instar larvae and 13 larvae in middle or later instars were individually inoculated in bamboo specimens and the amplitude of AE hits were recorded. The head capsule widths of the first instar larvae were measured before AE measurement. The specimens [15 (L) × 20 (T) mm] were prepared from a single air-dry madake internode [6 mm (R) thick]. A longitudinal hole with a depth of 5 mm was made on one end surface of each specimen using a push pin or drill bits (\varnothing 1.2–1.4 mm), depending on the larval body size, and a larva was placed in

this hole. This resulted in a larva-to-sensor distance of 10 mm. Each specimen was placed vertically on the face of the AE sensor, with the inoculated end surface on top, with a silicone grease as an acoustic couplant. AE measurement was conducted using the AE system (DiSP with AEwin) in the environmental chamber for at least 2 h after the larva started feeding. The mean value of 12 maximum amplitude values recorded in 10-min intervals during a 2-h period was calculated for each larva. This value is also referred to as mean maximum amplitude. After AE measurement, each of the middle or later instar larvae was extracted and killed in 99.5% ethanol. Because the head capsules of *D. minutus* larvae were partially hidden in the thoraces, except in the first instar, the head capsules of these extracted larvae were extruded from the thoraces to measure the widest part of the capsules.

4.2.6. Estimation of head capsule widths of all instars (Additional experiment IV)

Dyar (1890), who stated that the head capsule width of lepidopterous larvae follow a regular geometrical progression as they molt, recommended that the head capsule width of each instar be given in descriptions of larval stages. However, the larvae monitored inside the bamboo pieces could not be used to measure the head capsule width. Because the validity of Dyar's rule has been confirmed in various insect species including coleopteran species, such as the mountain pine beetle *Dendroctonus ponderosae* (Logan *et al.* 1998) and curculionid weevils *Sitona discoideus* (Frampton 1986) and *Pissodes castaneus* (Panzavolta 2007), his rule was applied to *D. minutus*. The head capsule widths of 20 newly hatched first instar larvae and 20 final instar larvae in the prepupal stage were measured, and the growth ratio and the head capsule width of each instar were calculated. As shown below, the number of instars varied

between seven and eight. Because the instar types of the prepupae were unknown, the head capsule width of each instar was estimated for both cases where the prepupae were all 7-instar type and 8-instar type.

4.3. Results and discussion

4.3.1. Feeding activity and development from the first instar to adult eclosion

Continuous generation of AE started within approximately 1 d after hatching. The AE hits detected from the bamboo pieces were attributable to larval feeding activity, based on Chapter 3, and even the activity of the smallest instar was detected. Considering the possibility of recording noise signals, the larvae were defined to be “active” when the hourly AE hit rate was 10 or higher, and otherwise they were regarded as being “inactive”. Figure 4.4 shows the time courses of the hourly AE hit rate and mean maximum amplitude of two individuals, A1 and AX1, as typical examples. They started continuous feeding at 0.6 d and 1.0 d, respectively. However, feeding activity ceased between 3.5 d and 5.5 d in individual A1 and between 5.2 d and 7.3 d in individual AX1, and after that, periods of continuous feeding activity and periods of inactivity alternated with each other.

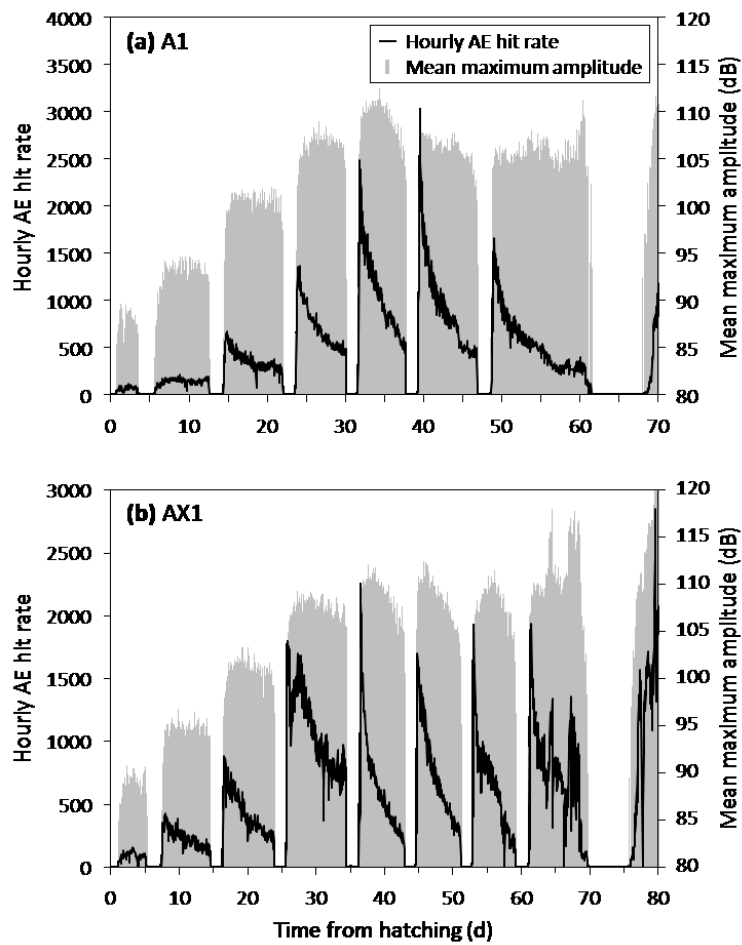


Fig. 4.4. Time courses of hourly AE hit rate and mean maximum amplitude of individuals A1 and AX1.

Direct observation (Additional experiment I) confirmed that these periods of inactivity that lasted for approximately 2 d were due to ecdysis. Figure 4.5 shows the process of ecdysis of a middle instar larva. Three instances of ecdysis were directly confirmed for three different larvae in middle or later instars. These larvae underwent ecdysis 1.1 d after they became inactive on average. They did not consume their skins. Two other instances of ecdysis of two first instar larvae were also captured, although both larvae died after ecdysis, probably because of the disturbance. Based on the direct observation, it was revealed that an active period corresponded to an instar period and the number of inactive periods represented the number of ecdysis events.

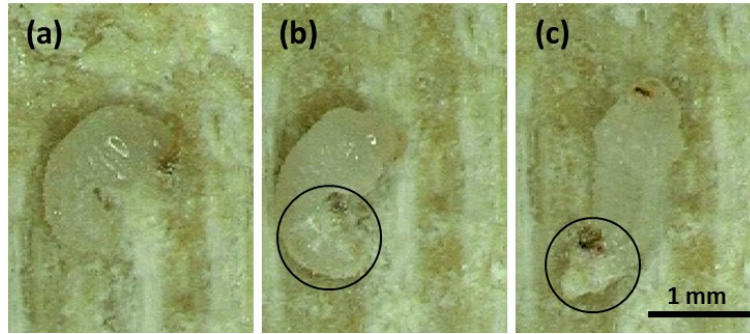


Fig. 4.5. Process of ecdysis of a larva. Exuvia is shown in *circles*. Image intervals are 300 s.

After completing the seventh instar, individual A1 entered a longer inactive period lasting from 61.5 d to 68.0 d (Fig. 4.4). Individual AX1 underwent an eighth instar before a long inactive period between 69.7 d and 75.7 d. Daily CT scans of individuals AX1 and AX2 confirmed that these periods corresponded to prepupal and pupal stages. Individual AX1 in the final instar became inactive at 69.7 d, and CT scans confirmed that it turned into a prepupa between 69.9 d and 71.0 d and pupated by 72.1 d. Direct observation of four final instar larvae showed that they pupated 1.5 d after they became inactive on average (Additional experiment I). Individual AX1 emerged as an adult between 74.9 d and 75.8 d. CT scans and AE measurement of individuals AX1 and AX2 suggested that adult beetles started feeding within approximately 1 d after eclosion. The feeding activity of adults is discussed in Subsection 4.3.4.

The time courses of the hourly AE hit rate in Fig. 4.4 showed that the larvae were most active shortly after completing ecdysis, and the activity reduced as the next ecdysis or pupation approached, in a certain instar after the third instar. The mean maximum amplitude of AE hits was rather constant in a certain instar. When compared among instars, both the hourly AE hit rate and mean maximum amplitude tended to increase with the instar number, suggesting that larger amounts of strain energy were released by the chewing movements of the mouthparts as the larval head and

mouthparts enlarged. However, after the fifth or sixth instar, these tendencies became less clear. These patterns of the time courses of the hourly AE hit rate and mean maximum amplitude were observed in all ten larvae. Possible reasons for these patterns were that the larvae were actually less active in later instars and/or that attenuation of AE waves became significant as the larvae moved away from the sensors. This matter is discussed in the next subsection with reference to the attenuation characteristics of the AE waves.

Figure 4.6 shows the progression of instars of all ten larvae, as well as the durations of instars, inactivity due to ecdysis, and prepupal and pupal stages. Five larvae underwent seven instars (“7-instar type”) and the other five underwent eight instars (“8-instar type”), suggesting that the number of instars can vary in this species. Variations in the number of larval instars were reported for related species, for example, the brown powderpost beetle *Lyctus brunneus* (Coleoptera: Bostrichidae) (Iwata and Nishimoto 1985) and the tobacco beetle *Lasioderma serricornis* (Coleoptera: Anobiidae) (Niiho 1984). Although other numbers of instars were not found in this study because of the limitation of the number of AE measurement channels, it is possible that other instar types of *D. minutus* were present, with low abundance ratios. The larval duration of 8-instar larvae was significantly longer than that of 7-instar larvae (Student’s *t*-test, $p < 0.01$). The adult body length was not significantly different between the instar types (Student’s *t*-test, $p > 0.05$), although the sample sizes may be too small to discuss differences among instar types. Sexual differences may be one of the factors causing the difference in the total number of instars. However, the sexes of the employed individuals were not identified in this experiment, limiting further discussion; the clarification of sexual differences in larval development is a subject for future analysis.

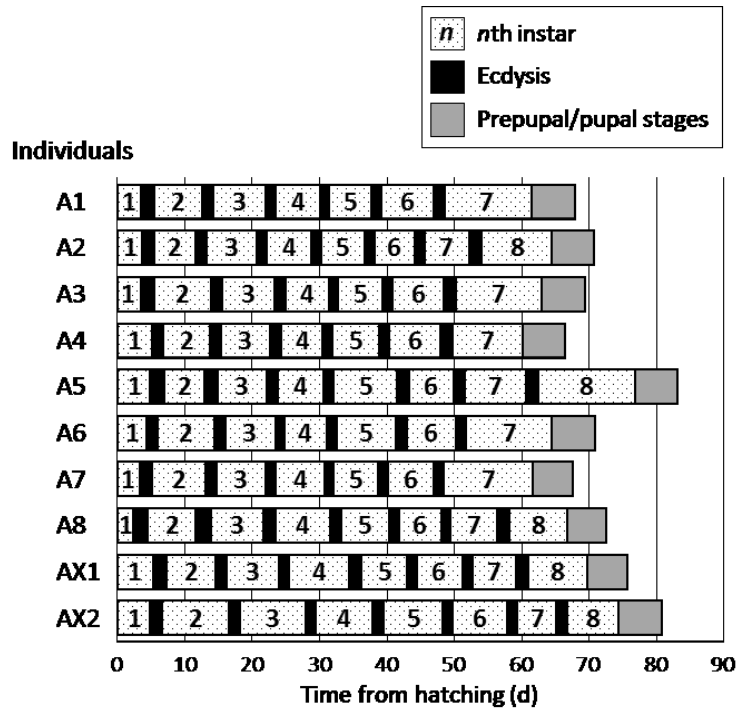


Fig. 4.6. Durations of larval instars, ecdysis, and prepupal/pupal stages.

The number of instars revealed in this study does not agree with previous reports on *D. minutus*. Plank (1948) estimated that *D. minutus* had four instars based on mandible lengths and Dyar's (1890) rule. Abood and Norhisham (2013) found five instars based on head capsule widths and inspection of exuviae, by rearing larvae individually using cassava flour. Garcia and Morrell (2009) reported that *D. minutus* larvae underwent four instars, but with no clear references to the methods of determining ecdysis. Some Japanese literatures (The Society of House and Household Pests Science, Japan 1995, Tokyo National Research Institute for Cultural Properties 2001, Yamano 1976) mention that *D. minutus* have five larval instars, but without presenting evidence. The differences between the results of this study and previous reports may be attributed to the accuracy of the conventional methods or to the variability of larval development among populations, regions, and rearing conditions. In addition, the results of this study showed that first instar was the shortest and the final

instars were the longest (Fig. 4.6), which was different from the report of Abood and Norhisham (2013) who found that the final instar was the shortest. The present results regarding larval development of *D. minutus* were rather similar to that of *D. ocellaris* reported by Sitaraman (1951). He reared *D. ocellaris* larvae using maize grain and found eight larval instars. The fact that the first instar was shorter than the other instars in *D. ocellaris* shown in his report also applied to *D. minutus* in this study. Although the present results were in disagreement with the previous reports on *D. minutus*, it was shown that AE monitoring was an effective novel tool for nondestructively assessing ecdysis and instars.

The average larval duration and prepupal/pupal duration of the ten individuals were 66.3 ± 5.7 d (mean \pm SD) and 6.2 ± 0.3 d, respectively. The average larval duration of the un-irradiated individuals, A1–A8, was 64.8 ± 5.3 d. This value was used in Chapter 2 to show that there was no impact of irradiation on developmental period of the larvae examined using X-ray CT. It should be noted that the larval durations measured from CT scanning and AE monitoring can be slightly different; in AE monitoring, the time from the end of feeding activity in the final instar to pupation, which was 1.5 d based on Additional experiment I, was not included in the larval duration.

As Fig. 4.4 shows, again, the hourly AE hit rate was constantly above a certain level during each instar, suggesting that the larvae were feeding continuously throughout. However, time courses of the number of AE hits with a higher temporal resolution exhibited the rhythmic presence of short phases of inactivity alternating with feeding phases. In insect physiology, such feeding phases preceded and followed by a “gap” are called “meals” (Bernays and Woods 2000, Nagata and Nagasawa 2006, Simpson 1982). A typical example is shown in the time course of the number of AE hits

per 5 min produced by individual A1 between 40 d and 40.5 d in Fig. 4.7a, where meals lasting approximately 40 min interchange with gaps of approximately 5 min. Figure 4.7b shows the FFT spectrum of the time course of AE hits per 5 min in the sixth instar, i.e., between 39.2 d and 46.9 d. In this spectrum, the highest peak is found at a frequency of 35.9 cycles/d, corresponding to a period of 0.67 h. This means that the activity of the larva had a dominant periodicity with a period of 0.67 h during the sixth instar. The distribution of intensity around the peak seemed skewed, with more components on the left (lower-frequency) side of the peak. The periods tended to lengthen as ecdysis approached and larval activity reduced, though this is not shown in Fig. 4.7a, and the shape of the distribution around the peak probably reflected this tendency. For simplification, the skewness is ignored in further discussion. Table 4.1 shows the average dominant period of periodic activity of each instar of all larvae. In the first and second instars, clear periodicity was not present except in the second instar of one individual. The periods of cycles tended to shorten as larval instars increased. The periods were much shorter than 24 h, suggesting that the feeding activity was independent of circadian rhythms, and the variation of periods within and among instars and individuals under constant conditions suggested that the rhythm in feeding activity was endogenous. Feeding patterns with a certain periodicity independent of circadian rhythms have been reported for nymphs and larvae of several insects, such as the migratory locust *Locusta migratoria* (Simpson 1982), tobacco hornworm *Manduca sexta* (Bernays and Woods 2000), and silkworm *Bombyx mori* (Nagata and Nagasawa 2006), and such patterns were estimated to be relevant to endogenous regulatory mechanisms (Nagata *et al.* 2011). Therefore, it is suggested that AE monitoring can also be applied to physiological analysis of the beetles.

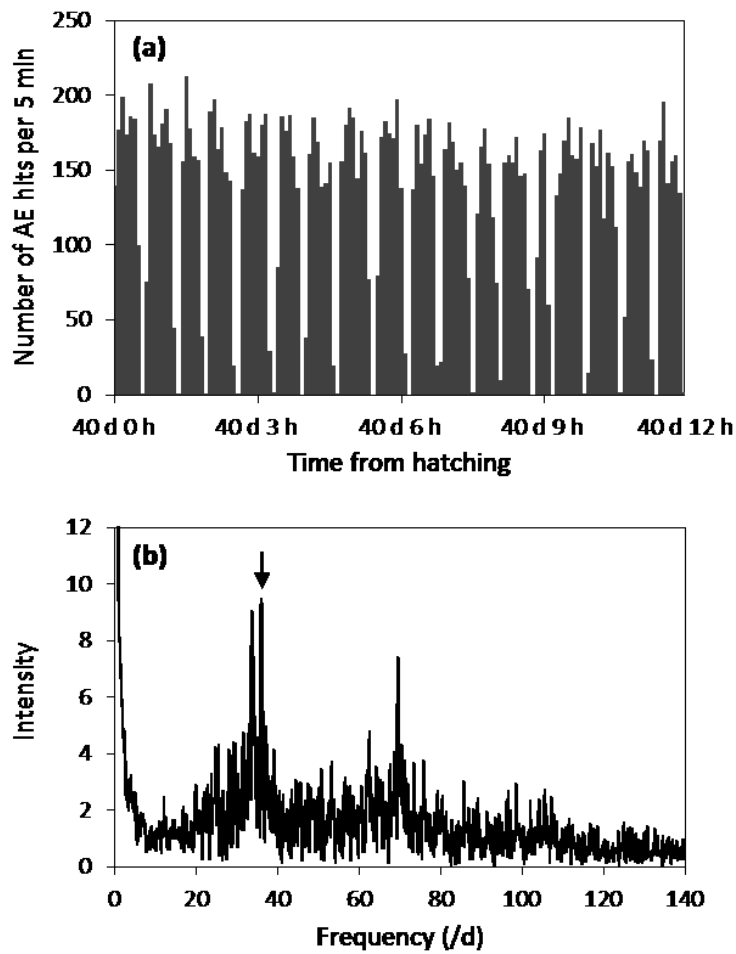


Fig. 4.7. Rhythmic pattern of feeding activity of individual A1. **a** Time course of the number of AE hits per 5 min between 40 d and 40.5 d after hatching. **b** FFT spectrum of the time course of the number of AE hits per 5 min during the sixth instar, i.e., between 39.2 d and 46.9 d. The highest peak, as indicated by an *arrow*, was found at the frequency of 35.9 cycles/d.

Table 4.1. Dominant period of the rhythms of feeding activity in each larval instar, averaged over ten individuals ($n = 10$) except where noted.

Instar	Period (mean \pm SD) (h)
1	ND
2	2.19 ($n = 1$)
3	2.04 \pm 1.16
4	1.15 \pm 0.31
5	0.97 \pm 0.32
6	0.76 \pm 0.13
7 (of 7-instar larvae)	0.80 \pm 0.10 ($n = 5$)
7 (of 8-instar larvae)	0.77 \pm 0.13 ($n = 5$)
8	0.86 \pm 0.11 ($n = 5$)

SD standard deviation, *ND* not detected

In summary, AE monitoring was an effective tool for nondestructively detecting real-time feeding activity of *D. minutus* and determining the number of ecdysis events, the duration of instars, and larval and pupal developmental periods. It should be applicable to other bamboo- and wood-boring insects as well. Real-time analysis using AE also indicated the presence of rhythms in the temporal transitions of feeding activity within each instar period, which may reflect the endogenous regulatory mechanisms of the larvae.

4.3.2. Effects of attenuation of AE waves

In the previous subsection, it was noted that the hourly AE hit rate and mean maximum amplitude did not increase with larval instars after the fifth or sixth instar (Fig. 4.4), and it was discussed that the reasons for these patterns may be that the larvae were actually less active in later instars and/or that attenuation of AE waves became

significant as the larvae moved away from the sensors. In order to examine the extent of attenuation in the experimental conditions of this study, the distance attenuation of elastic waves propagating longitudinally in bamboo culms was measured (Additional experiment II), and the AE data of individuals AX1 and AX2 were corrected using the attenuation value. Figure 4.8 shows the relationship between the propagation distance and amplitude level of 150-kHz output signals for one bamboo specimen. The amplitude level decreased linearly with propagation distance, and the slope of the regression line was -0.12 . The average longitudinal attenuation of three specimens, at 8–9% MC, was 0.11 dB/mm. Therefore, it was estimated that the amplitude of AE waves in bamboo culms decrease nearly by this value when using AE sensors with a resonant frequency of 150 kHz.

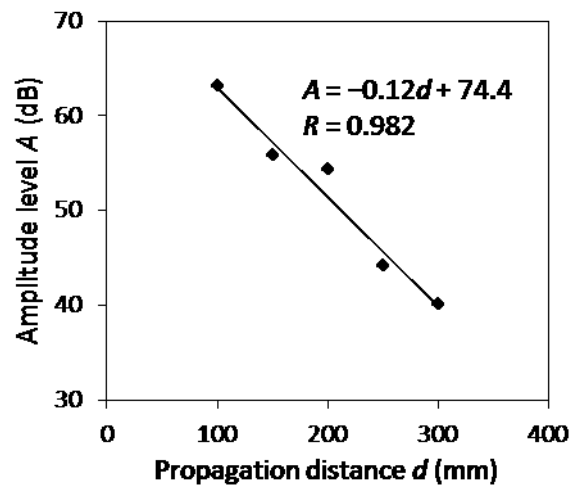


Fig. 4.8. Relationship between propagation distance and the amplitude level of output signals of 150-kHz elastic waves.

The AE data of individuals AX1 and AX2 were then corrected based on the distance attenuation measured in Additional experiment II. The amplitude of each AE hit at the source was estimated by compensating for attenuation, using an attenuation value of 0.1 dB/mm and the supposed propagation distance based on the linear

interpolation of the distance between the larva and the sensor measured in X-ray CT images. The corrected AE hits were discriminated at a new threshold of 90 dB. Figure 4.9 shows the time courses of corrected hourly AE hit rate and mean maximum amplitude of individual AX1. Both of these AE parameters increased with each instar, although the hourly AE hit rate at the beginning of the fifth instar was an exception for unknown reasons. Similar patterns were observed for individual AX2 as well. The correction based on attenuation indicated that the amplitude of AE waves, and thus the number of detectable signals (AE hits), always increased as the larvae underwent ecdysis events although this tendency became seemingly unclear after the fifth or sixth instar solely because of the attenuation of AE waves.

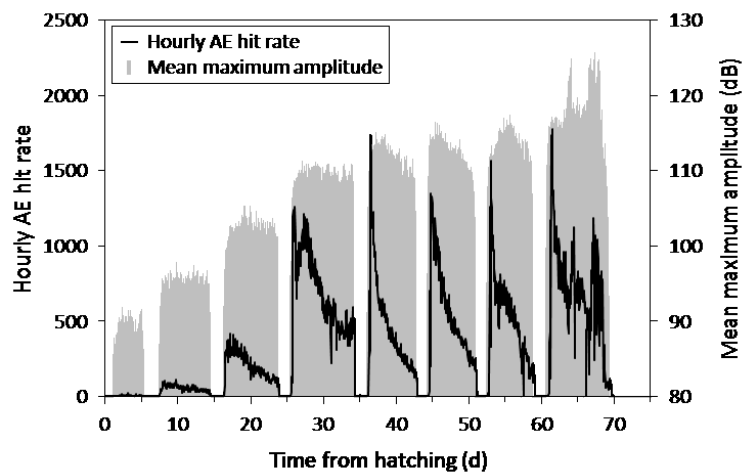


Fig. 4.9. Time courses of corrected hourly AE hit rate and mean maximum amplitude of individual AX1. The correction was based on the estimated attenuation of AE waves and the distance between the larva and the sensor.

In order to further clarify the relationship between larval instars and produced AE amplitude, AE signals generated by larvae of different instars were measured with a fixed propagation distance of 10 mm in Additional experiment III. Then, the head capsule widths of the larvae, except the four first instar larvae, were measured to estimate their instars. For instar estimation, a lookup table (Table 4.2) showing head capsule width of each instar calculated from 20 first instar larvae and 20 final instar larvae was made in Additional experiment IV. This table lists the measured head capsule widths of the first and final instars, growth ratios calculated based on Dyar's (1890) rule, and calculated head capsule widths of intermediate instars for both 7- and 8-instar types. Figure 4.10a shows the relationship between the head capsule width of larvae and mean maximum amplitude, the original result of Additional experiment III. Figure 4.10b, c shows the relationship of mean maximum amplitude to larval instars, estimated based on Table 4.2 using the arithmetic means of head capsule widths of consecutive instars as borders. All of the correlations ($R = 0.926$, 0.974 , and 0.973 for Fig. 4.10a–c, respectively) were significant ($p < 0.01$), meaning that AE amplitude increased with larval head size and each instar. In addition, because the patterns in which maximum amplitude did not increase with each instar were only observed after the fifth or sixth instar, regression analysis was applied only to the mean maximum amplitude values of the fifth and later instars. The correlations ($R = 0.788$ and 0.817 for Fig. 4.10b, c, respectively) were significant ($p < 0.01$) in both instar types. Therefore, it was confirmed that the amplitude of AE waves at their sources increased with head capsule width and the instar number.

Table 4.2. Estimated head capsule width of each larval instar.

Instar	7-instar type		8-instar type	
	Head capsule width (mm)	Growth ratio r	Head capsule width (mm)	Growth ratio r
1	0.119*		0.119*	
2	0.160		0.153	
3	0.215		0.198	
4	0.290	1.35**	0.255	1.29**
5	0.390		0.329	
6	0.524		0.424	
7	0.706*		0.547	
8	–		0.706*	

* Mean of 20 measured values

** Calculated from measured head capsule widths of the first and final instars (*) based on Dyar's rule

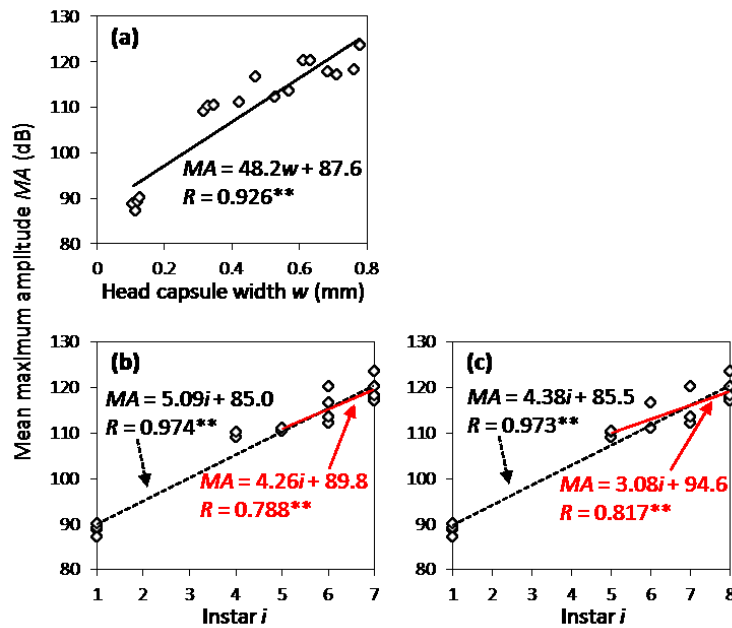


Fig. 4.10. Relationship between head capsule width of larvae and mean maximum amplitude (a) and relationship between larval instars and mean maximum amplitude on the assumption that the larvae were of 7-instar type (b) and 8-instar type (c). Dashed lines in b and c are the regression lines using values of all instars, and red solid lines are the regression lines using values between the fifth and final instars. Two asterisks (**) denotes that the correlation is significant at the 0.01 level.

Overall, it was shown that, when the larvae moved far away from the sensor, attenuation of AE waves became so significant that the larval activity could be underestimated. By compensating for attenuation, the correlation of AE amplitude with larval instars became clearer, reflecting the growth of the larvae. In the application of AE monitoring for continuous analysis of feeding by bamboo- and wood-boring insects, attenuation may not be problematic in separating instar periods from inactivity due to ecdysis or even in separating meals and subsequent (or preceding) gaps as long as the rearing media are of confined dimensions. However, when quantitatively comparing the level of feeding activity of different instars or individuals, it is desirable that the attenuation characteristics be evaluated in some manner, such as demonstrated in Additional experiment II.

4.3.3. Relationship between cumulative AE hits and bamboo consumption

In Chapter 3, the relationship between the movements of the mandibles of *D. minutus* and AE generation was clarified. However, the AE phenomenon is yet to be related to the actual amount of bamboo consumption by the larvae. In this subsection, the relationship between the number of AE hits and bamboo consumption is discussed using individuals AX1 and AX2. The tunnel volumes measured using X-ray CT images were used to represent bamboo consumption. The tunnel volume bored during each instar was estimated assuming that the tunnel volume increased linearly with time between two CT scanning dates and that the larvae did not extend tunnels during inactive periods of ecdysis. Figure 4.11 shows the relationship between cumulative AE hits (after correcting based on attenuation) and tunnel volume recorded from hatching until the end of each instar for the two larvae. The graphs in Fig. 4.11 confirm that the

bamboo consumption increased as more AE hits were produced, although the relationship did not seem to be linear. A possible explanation for the rather concave shape of these curves was the growth of the mandibles; as the larvae enlarged through ecdysis events, larger amounts of bamboo were consumed by one bite of the mandibles. In addition, each of the two larvae consumed a total of 68.1 mm³ of bamboo on average, and the average percentage of bamboo consumption in each instar from first to eighth was 0.03, 0.3, 1.0, 2.2, 6.0, 14, 27, and 49%, respectively. This indicated that bamboo consumption increased greatly with each instar and suggests that detection and treatment in early larval instars would significantly reduce the damage caused by the larvae.

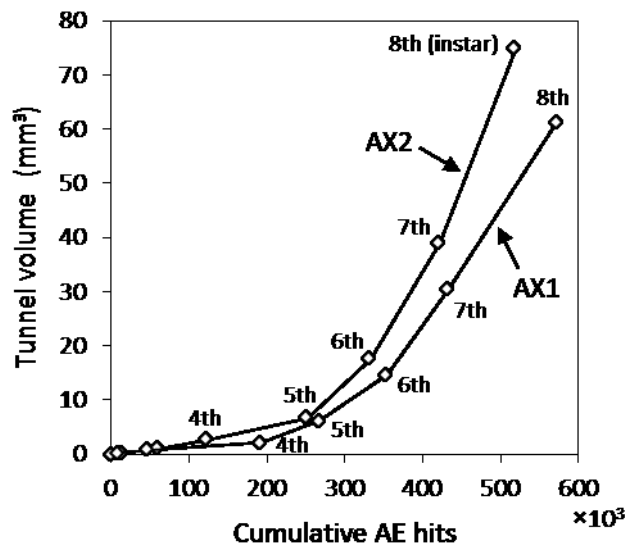


Fig. 4.11. Relationship between cumulative AE hits (corrected based on attenuation) and tunnel volume recorded from hatching until the end of each instar. *Ordinal numbers* represent instar numbers, excluding the first to third instars.

4.3.4. Pre-mating adult feeding activity

Analysis of pre-mating adult feeding (Reifungsfrass) was continued for approximately 10 d because, as described in Chapter 2, adults made exit holes in 8 d after adult eclosion on average. Figure 4.12 shows the time courses of the hourly AE hit rate and mean maximum amplitude of individual A1, in continuation of Fig. 4.4a. It should be noted that a higher threshold value was employed for adult monitoring, so the adult hourly AE hit rate is not comparable with the larval data. As mentioned in Subsection 4.3.1, adults were considered to have started feeding within approximately 1 d after eclosion. Figure 4.12 indicates that feeding activity continued almost ceaselessly during Reifungsfrass, although it was relatively low for 1–2 d after the adults started feeding. Adults produced AE waves of larger amplitude than the final instar larvae. Unlike larval feeding, there was no clear periodicity in the time courses of the number of AE hits per 5 min.

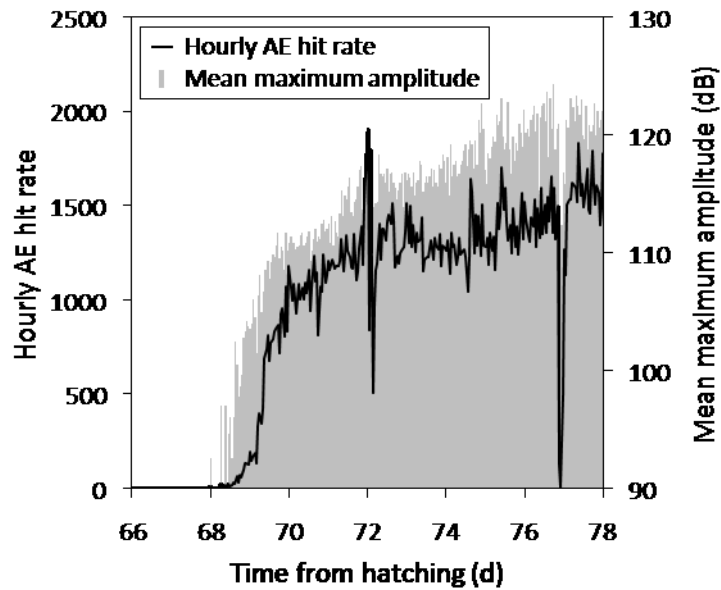


Fig. 4.12. Time courses of hourly AE hit rate and mean maximum amplitude after adult eclosion of individual A1. It should be noted that, because a higher threshold value was employed, the adult hourly AE hit rate is not comparable with the larval data shown in Fig. 4.4.

4.4. Summary

AE monitoring was used to analyze larval feeding and development of *D. minutus* from the first instar. AE hits produced by feeding activity were detected, and the larvae showed almost constant feeding activity every hour during the instar periods but became inactive during periods of ecdysis and pupation. Therefore, AE monitoring proved to be an effective tool for measuring larval duration and the number of ecdysis events. The examined larvae underwent either seven or eight instars in total, which differed from previous reports on *D. minutus*. The AE data also indicated the presence of periodicity in larval feeding; continuous meals were separated by short inactive

phases (approximately 5 min), with an average dominant period in each instar ranging between 0.76 and 2.19 h, which possibly reflected the physiology of the larvae. The AE amplitude increased with each larval instar, but because of the attenuation of AE waves, this relationship became unclear in later larval stages without additional corrections. Bamboo consumption increased as cumulative AE hits increased, and the non-linear relationship between these suggested that more bamboo was consumed by each bite as the larval instars progressed. The feeding activity of newly emerged adults continued almost ceaselessly, based on hourly AE hit rate, in the Reifungsfrass period. These results show that another novel nondestructive methodology for the analysis of feeding and development of *D. minutus* has been established.

Chapter 5. General discussion and future perspectives

5.1. Introduction

This research was designed with the consideration that nondestructive techniques for detecting and analyzing the development and feeding of bamboo-boring insects are essential in establishing measures of prevention, remediation, and inspection to manage insect attack to bamboo materials. The use of two particular techniques, X-ray computed tomography (CT) and acoustic emission (AE) monitoring, in evaluating larval development and feeding of the bamboo powderpost beetle *Dinoderus minutus* was investigated in the experiments described in Chapters 2–4. In this chapter, the novelty of these techniques and findings revealed by them is confirmed from the entomological point of view. Then, it is discussed how X-ray CT and AE monitoring could be utilized and contribute to the establishment of integrated pest management (IPM) for bamboo materials.

5.2. Novelty of monitoring using X-ray CT and AE in entomology

Nondestructive analyses by X-ray CT and AE monitoring provided understanding regarding the growth and development of *D. minutus*, such as changes in body size, the number and time period of instars, and larval and pupal developmental periods. Although these points have been reported previously, conventional methods employed in previous studies involved either the direct dissection of bamboo culms used for rearing (Garcia and Morrell 2009, Norhisham *et al.* 2015, Plank 1948) or the use of artificial diets (Norhisham *et al.* 2013). X-ray CT and AE monitoring were effective tools for clarifying the process of beetle development in natural conditions in a relatively simple manner. In addition, they could now be used to examine differences, if

any, between larval development in bamboo culms and that in artificial diets.

X-ray CT and AE monitoring also revealed information regarding the characteristics of feeding, such as 3D tunneling patterns and temporal transitions in feeding activity. Quantifying the amount of bamboo consumed by the larvae would be particularly difficult using other methods, and it was first attained using X-ray CT. Real time monitoring of feeding activity, as well, was first made possible using AE. The rhythmic patterns of feeding activity found through AE monitoring may be related to the physiology of the larvae. In the field of insect physiology, continuous observation of feeding and other activities of insects was conducted to study the mechanism of the rhythms in feeding and factors influencing these rhythms (Bernays and Woods 2000, Nagata and Nagasawa 2006, Simpson 1982). AE monitoring may be a useful tool to analyze the physiology of the beetles. Furthermore, although not found in larval feeding activity, AE data could also be used to detect circadian rhythms in beetle activities. In this case, AE hit rate, the number of AE hits detected in a certain unit of time, could be directly input to compute the chi-square periodogram, which determines the circadian period and its statistical significance (Sokolove and Bushell 1978).

X-ray CT and AE monitoring are also promising for analysis of the ovipositional behavior of *D. minutus*. Because adult *D. minutus* lay eggs along oviposition tunnels made by themselves (Plank 1948, Ueda 1963, Wood Technological Association of Japan 1961, Yamano 1976), direct observation of this behavior is very difficult, and related facts, such as the number of eggs laid per female in bamboo culms and the extent of damage caused during the ovipositional period, are poorly understood. In the experiments in progress by the author, it was confirmed that eggs laid in bamboo vascular bundles could be visualized by X-ray CT (Watanabe *et al.* 2017c). Other activities of adult males and females can be directly observed when they are outside of

bamboo culms, but it is generally known that they are only active outside toward evening (Plank 1948), and they are mostly hidden inside bamboo culms. X-ray CT and AE monitoring, combined with direct observation of activities outside, could comprehensively clarify the activity patterns of adult beetles, revealing the entire life history and feeding behavior in all life stages.

Some of the findings were only revealed by either X-ray CT or AE monitoring, for example, tunnel volume by the former and instars and ecdysis events by the latter, and their interrelationship was clarified using the combination of the two techniques. However, in circumstances where only either one of these techniques is available, X-ray CT could be devised to estimate the conditions of larval development or feeding previously revealed solely by AE monitoring, and vice versa. For example, considering that the inactive periods due to ecdysis lasted approximately 2 d, ecdysis events may be estimated by CT scans at 1- or 2-day intervals, and bamboo consumption could be estimated from cumulative AE hits once their relationship is clarified, as in Fig. 4.11.

Therefore, X-ray CT and AE monitoring are novel, effective tools to nondestructively study the biology, especially the life history and feeding behavior, of *D. minutus* in bamboo culms. These tools are also considered to be applicable for the analysis of other bamboo- and wood-boring insects.

5.3. Usefulness of X-ray CT and AE monitoring in managing *D. minutus*

5.3.1. Desirable process of IPM for bamboo materials

As explained in “General introduction”, there are two possible ways in which infestations of bamboo-boring insects occur. The entrance of beetles in the manufacturing process must be detected before being put into use. This may be

attempted visually, but more reliable methods of detection are desirable. When the presence of live beetles is detected, the bamboo culms could be treated with a remedial measure. Whether or not the culms had been infected, preventive measures should be applied before being made into products or integrated into constructions. Infestations that occur in bamboo culms in use should be detected in the early stage by regular inspection using a reliable apparatus. Damaged parts should be processed using a remedial measure or be disposed of and replaced, and the application of preventive measures is necessary to prevent re-infestation. Therefore, development of reliable, preferably nondestructive detection systems and appropriate preventive and remedial measures is needed. General chemical and physical control methods for the prevention and remediation of insect pests that may be applicable to bamboo-boring beetles are summarized in Table 5.1.

Table 5.1. Typical examples of pest control methods, based on Kamimura and Moriyama (2004) and Saito *et al.* (1986)

Purpose	Chemical control	Mechanical/physical control
Remediation	Use of insecticides	Trapping/catching, including uses of light and adhesive traps
	Mass trapping using attractants	Heating
	Use of growth regulators	Chilling
Prevention	Inhibition of infestation Increasing of materials' resistance to pests Inhibition of mating	Sterilization
	Evasion of attack	Use of repellents Blocking

There are two ways in which X-ray CT and AE monitoring could be utilized in the management of bamboo-boring beetles. They could be used as control measures,

and they could be used as laboratory analysis tools to obtain information required for developing control measures. Applications in both ways are discussed in the following subsections with *D. minutus* as an example of a bamboo-boring beetle species.

5.3.2. Application of X-ray CT and AE to inspection of insect attack

The principles of X-ray CT and AE monitoring are applicable to nondestructive inspection of bamboo culms to determine the presence of insect damage and active insects, whether application of a remedial treatment is necessary, whether the damaged culms have enough residual strength to be reused, and whether the remedial treatments applied to infested culms have been effective.

Inspection using X-ray CT could accurately reveal the number and developmental stages of beetles present and extent of damage in infested culms. Repeated scans at certain intervals may be needed to confirm whether the beetles inside are active or not. The scanning conditions of the protocols employed in Chapter 2 can be the basis for inspection using X-ray CT. In order to be able to estimate the residual strength of attacked culms, the relationship with the extent of damage needs to be clarified.

The waveforms of AE signals generated by *D. minutus* in Chapter 3, the relationship between the amplitude and developmental stages clarified in Chapter 4, and the distance attenuation of elastic waves in bamboo culms measured in the same chapter are useful in interpreting signals detected from possibly infested culms; they may be used to determine whether the signals result from active beetles or from other sources, estimate the severity of attack, and determine the appropriate intervals of measurement points to place sensors. For example, supposing the measurement system employed in

the main experiment described in Chapter 4, when a final instar larva produced an AE wave with amplitude of 120 dB, it would propagate approximately 0.4 m before attenuating to the threshold level of 80 dB. The presence of rhythms in larval feeding activity may also be useful in differentiating feeding activity from sporadic or stationary noise signals. Because of the inactivity due to ecdysis or pupation, AE monitoring may need to be continued for several days even if AE signals are not detected.

The systems for X-ray CT scanning and AE measurement employed in the present research could be directly used in laboratory inspection of damaged bamboo objects or parts. On the other hand, the development of apparatuses for *in situ* detection that could be used, for example, in a construction should be pursued in the future. Portable AE devices employed for termite detection in wooden constructions (Fujii *et al.* 1998, Yanase *et al.* 1999, 2001) may be applicable, but optimization of the devices to bamboo culms, which have hard, round surfaces and different acoustic characteristics than ordinary wood, is necessary.

5.3.3. Application of X-ray CT and AE as laboratory analysis tools in developing control measures

X-ray CT and AE monitoring, as laboratory analysis tools, can contribute to the management of *D. minutus* in two ways. They can be used to evaluate the efficacy of preventive and remedial treatments and to reveal entomological knowledge on which the development of control measures is based.

An example of the former application could be the investigation of optimum conditions for chemical and physical remedial treatments by detecting the termination of activity, death, or resumption of activity. The conditions include the concentrations of active chemical ingredients in chemical treatments or fumigation, and the time and

temperatures required in heat and chilling treatments. Because *D. minutus* prefer bamboo culms slightly moister than in air-dry conditions (Norhisham *et al.* 2015, Ueda 1963, Wood Technological Association of Japan 1961, Yamano 1976), curing at low humidity might be another non-chemical remedial treatment that should be investigated for its effectiveness. Real-time analysis using AE monitoring would be especially suitable in such investigations. In addition, AE measurement could reveal the threshold temperature for feeding activity to start, which would be important for *in situ* inspection using AE monitoring at low temperatures. AE monitoring could also be used to evaluate the development- and ecdysis-inhibiting efficacy of certain remedial treatments, such as use of chemicals or irradiation. Furthermore, the efficacy of methods of mating disruption and sterilization could probably be evaluated by tracing the ovipositional behavior of treated females using X-ray CT.

Entomological facts of *D. minutus* that were or could be revealed by X-ray CT and AE monitoring could be utilized in IPM as explained below.

Knowing the number of instars is important in remedial treatments. The efficacy of remedial treatments, such as chemical and heat treatments, may be different at various stages. The conditions necessary to kill individuals in various instars could be evaluated by X-ray CT and AE monitoring. Clarification of appropriate conditions could prevent excessive application of treatments, reducing the cost, negative impacts on treated bamboo materials, human health, and environment, and the risk of beetles' acquiring tolerance to active chemicals.

In this research, the durations of egg, larval, and pupal developmental periods of *D. minutus* and their bamboo consumption during the larval stages under constant conditions were determined. However, these durations and amounts are likely to vary under different conditions, and X-ray CT and AE monitoring could be used to

investigate the effects of various factors on developmental periods and bamboo consumption. In general, a linear relationship is satisfied between the reciprocal of a developmental period (rate of development) of an insect and the temperature at which development occurs, and this relationship is characterized by two constants, low developmental threshold temperature and thermal constant. Investigation of the developmental durations at different temperatures could reveal the two constants for each stage. The deduced relationship between temperature and developmental period, which allows estimation of the developmental duration at any temperature, would be useful in any circumstances for IPM, for example, for estimating the emergence of the next generation when there is a possibility of re-infestation or estimating the time period elapsed after the first entrance of mother beetles.

The extent of attack caused by the larvae, which was evaluated in terms of tunnel length and volume, may also be a function of various conditions, for example, nutritional conditions of the bamboo culms. Because the contents of starch and other carbohydrates in bamboo culms fluctuate throughout the year, studies have been conducted to quantify the fluctuation of the contents of starch and sugars throughout the year (Garcia and Morrell 2008, Hirano *et al.* 2003, Okahisa *et al.* 2006, Yoshimoto and Morita 1985) and to clarify the relationship of the contents of carbohydrates to the extent of attack of *D. minutus* (Garcia and Morrell 2008, Plank and Hageman 1951). However, only adult entrance was observed in these studies, and other aspects of the life history such as the number of eggs laid inside culms or damage caused by the developing larvae were not examined. X-ray CT and AE monitoring could be used to investigate the effects of nutritional factors on oviposition, larval development, and extent of attack during these processes. The results could provide a method to estimate the susceptibility of bamboo culms and be applied to developing novel treatments to

increase the resistance of bamboo culms. In addition, laboratory efficacy tests of chemical preventive treatments were evaluated based on adult entrance into culms in previous studies (Garcia and Morrell 2010, Ninomiya and Kotani 2002, Plank 1950). X-ray CT and AE monitoring could also be used to evaluate the efficacy of these treatments in reducing the amount of damage caused during ovipositional and developmental processes. Furthermore, once the effects of environmental and nutritional conditions on development and feeding are comprehensively clarified, a reliable model predicting the progress of infestation and resultant damage to bamboo culms could be designed.

In Section 5.2, it was explained that X-ray CT and AE monitoring are promising for investigating the ovipositional behavior and other activities of adults. Characteristics of oviposition should be considered when developing methods for inhibiting oviposition, one of the most important keys to protecting bamboo materials. Understanding the comprehensive patterns of adult activities, such as oviposition, feeding, and quiescence inside and flight and mating outside, may also facilitate the development of control measures relevant to adult behavior, including trapping, mating-inhibition, repelling, and blocking.

Understanding regarding the life history and feeding of *D. minutus* obtained in this research may not directly be used to implement IPM, but further investigation of *D. minutus* using X-ray CT and AE monitoring could provide information valuable for developing control measures, such as shown in Table 5.1, leading to the establishment of IPM for bamboo materials.

Summary and conclusions

The susceptibility of felled bamboo culms to insect attack is an important factor limiting their widespread use. The bamboo powderpost beetle *Dinoderus minutus* is a major insect pest of bamboo culms. This research was conducted to evaluate the applicability of X-ray computed tomography (CT) and acoustic emission (AE) monitoring for nondestructive evaluation of larval development and feeding of *D. minutus* in bamboo culms.

In Chapter 1, it was revealed by literature review that the life history and feeding biology of *D. minutus* were poorly understood because of the difficulty observing and analyzing the beetles inside bamboo culms, and nondestructive techniques appropriate for such usage were needed.

In Chapter 2, X-ray CT was shown to be an effective tool to nondestructively and quantitatively evaluate the growing body size and extending tunnel size of *D. minutus*. The larval tunnels reached 80.2 mm in length and 68.0 mm³ in volume on average. In Chapter 3, it was directly confirmed that AE waves were generated by the feeding activity of *D. minutus* based on direct observation of the mandibles of *D. minutus* and AE measurement, suggesting that AE measurement could be used for continuous, real-time monitoring of feeding activity. In Chapter 4, it was shown that AE monitoring was useful for nondestructively determining instar periods and ecdysis events and analyzing rhythms in feeding activity. The larvae underwent seven or eight instars in total. With a combination of X-ray CT and AE monitoring, the relationship between the amount of bamboo consumption and the number of AE hits was clarified.

In Chapter 5, the significance of the techniques and obtained results was discussed. The discussion draws the conclusions that X-ray CT and AE monitoring are

novel, effective tools to nondestructively study the biology of *D. minutus*, and that these techniques will contribute to the integrated pest management for bamboo materials, both directly as inspection tools and indirectly through monitoring and analysis of insect biology.

Acknowledgements

I would like to express my deepest gratitude to Professor Dr. Yoshihisa Fujii, Laboratory of Wood Processing, Division of Forest and Biomaterials Science, Graduate School of Agriculture, Kyoto University, for supervising my research for six years. I owe my research achievements to his kind support, advice, and encouragement throughout the years.

I would like to express my sincere gratitude to Professor Dr. Tsuyoshi Yoshimura, Laboratory of Innovative Humano-habitability, Research Institute for Sustainable Humanosphere, Kyoto University, and Professor Dr. Kenji Matsuura, Laboratory of Insect Ecology, Division of Applied Bioscience, Graduate School of Agriculture, Kyoto University, for reviewing the manuscript of this thesis and giving critical comments.

I would like to express my sincere gratitude to Assistant Professor Dr. Yoshiyuki Yanase, Laboratory of Wood Processing, Division of Forest and Biomaterials Science, Graduate School of Agriculture, Kyoto University, for his continued support of my research and technical help in conducting experiments.

I would like to thank Assistant Professor Yutaka Sawada and Researcher Dr. Yuko Fujiwara, Laboratory of Wood Processing, Division of Forest and Biomaterials Science, Graduate School of Agriculture, Kyoto University, for their technical support.

I would also like to thank the members and former members of Laboratory of Wood Processing, Division of Forest and Biomaterials Science, Graduate School of Agriculture, Kyoto University, for supporting my laboratory life from 2012 to 2018.

December 2017
Hiroki Watanabe

References

- Abood, F., Norhisham, A. R. (2013) Larval development of the bamboo borer (*Dinoderus minutus* Fabricius) using individual rearing method. *Pertanika Journal of Tropical Agricultural Science* **36**(S), 55–66.
- Abood, F., Norhisham, A. R., Shahman, M., Andy, A. (2010) Sexual identification of bamboo borer *Dinoderus minutus* (Fabricius) (Coleoptera: Bostrychidae). *Malaysian Forester* **73**(1), 1–6.
- Acda, M. N. (2008) Insecticidal activity of thiamethoxam against the bamboo powder post beetle *Dinoderus minutus* Fabr. (Coleoptera: Bostrichidae). *Journal of Pest Science* **81**(2), 109–113.
- Amman, G. D., Rasmussen, L. A. (1969) Techniques for radiographing and the accuracy of the X-ray method for identifying and estimating numbers of the mountain pine beetle. *Journal of Economic Entomology* **62**(3), 631–634.
- Baba, Y., Ainara, K. (2014) Development of control method for powder post beetle: examination of inducing oviposition method and evaluation of inhibition efficacy of pesticides for oviposition and hatching (in Japanese). *Mokuzai Hozon (Wood Protection)* **40**(2), 64–69.
- Bélanger, S., Bauce, E., Berthiaume, R., Long, B., Labrie, J., Daigle, L. F., Hébert, C. (2013) Effect of temperature and tree species on damage progression caused by whitespotted sawyer (Coleoptera: Cerambycidae) larvae in recently burned logs. *Journal of Economic Entomology* **106**(3), 1331–1338.
- Bernays, E. A., Woods, H. A. (2000) Foraging in nature by larvae of *Manduca sexta*—influenced by an endogenous oscillation. *Journal of Insect Physiology* **46**(5), 825–836.
- Berryman, A. A., Stark, R. W. (1962) Radiography in forest entomology. *Annals of the Entomological Society of America* **55**(4), 456–466.
- Bletchly, J. D. (1960) Studying the eggs of *Lyctus brunneus*. *Timber Technology* **68**(2247), 29–31.
- Brooks, S. E., Oi, F. M., Koehler, P. G. (2003) Ability of canine termite detectors to locate live termites and discriminate them from non-termite material. *Journal of Economic Entomology* **96**(4), 1259–1266.
- City of Nagoya (2009) Nagashinkuimushi-rui ni tsuite (About bostrychid beetles) (in Japanese). <http://www.city.nagoya.jp/kenkofukushi/page/0000004820.html>. Accessed 24 November, 2017.
- Creemers, J. G. M. (2013) Use of Acoustic Emission (AE) to detect activity of common European dry-woodboring insects: some practical considerations. Proceedings of IRG Annual Meeting 2013, Stockholm, Sweden, IRG/WP 13-10803, 8 pp.
- Creemers, J. G. M. (2015) Use of acoustic emission (AE) to detect activity of common European dry-woodboring insects: practical considerations. Proceedings of the International Symposium Non-Destructive Testing in Civil Engineering 2015, Berlin, Germany, 8 pp.
- Dyar, H. G. (1890) The number of molts of lepidopterous larvae. *Psyche* **5**(175–176), 420–422.
- Evans, T. A. (2002) Assessing efficacy of TermatracTM; a new microwave based technology for non-destructive detection of termites (Isoptera). *Sociobiology* **40**(3), 575–583.
- Fisher, R. C., Tasker, H. S. (1940) The detection of wood-boring insects by means of X-rays. *Annals of Applied Biology* **27**(1), 92–100.

- Fisher, W. S. (1950) A revision of the North American species of beetles belonging to the family Bostrichidae. (Miscellaneous Publication No. 698), United States Department of Agriculture, Washington, D. C., pp. 24–33.
- Follett, P. A. (2004) Irradiation to control insects in fruits and vegetables for export from Hawaii. *Radiation Physics and Chemistry* **71**(1–2), 161–164.
- Forestry Agency (2011) Take-kankei-shiryō (Information related to bamboo) (in Japanese). <http://www.rinya.maff.go.jp/j/tokuyou/tokusan/megurujoukyou/pdf/4take.pdf>. Accessed 27 November, 2017.
- Forestry and Forest Products Research Institute (ed.) (2004) Mokuzai-kōgyō handbook (Handbook for wood industry) (4th edition) (in Japanese). Maruzen, Tokyo, pp. 194–195.
- Frampton, E. R. (1986) Determination of the number of larval instars of *Sitona discoideus* Gyllenhal (Coleoptera: Curculionidae) using probit analysis. *New Zealand Journal of Zoology* **13**(1), 107–111.
- Fuchs, A., Schreyer, A., Feuerbach, S., Korb, J. (2004) A new technique for termite monitoring using computer tomography and endoscopy. *International Journal of Pest Management* **50**(1), 63–66.
- Fujii, T. (ed.) (2013) Basic science and advanced technologies for industrial applications of bamboo (popular edition) (in Japanese). CMC Publishing, Tokyo, 236 pp.
- Fujii, Y., Fujiwara, Y., Yanase, Y., Okumura, S., Narahara, K., Nagatsuma, T., Yoshimura, T., Imamura, Y. (2007) Nondestructive detection of termites using a millimeter-wave imaging technique. *Forest Products Journal* **57**(10), 75–79.
- Fujii, Y., Imamura, Y., Iwatsubo, E., Yamamoto, S. (1997) Control of termite attack using trapping method and acoustic emission (AE) monitoring: a case study at an electric power plant (in Japanese). *Mokuzai Hozon (Wood Protection)* **23**(3), 111–120.
- Fujii, Y., Imamura, Y., Shibata, E. (1994) Detection of acoustic emission (AE) generated by the feeding activity of *Semanotus japonicus* LACORDAIRE (in Japanese). *Japanese Journal of Environmental Entomology and Zoology* **6**(3), 112–118.
- Fujii, Y., Imamura, Y., Shibata, E., Noguchi, M. (1992) Feasibility of AE (Acoustic Emission) monitoring for the detection of the activities of wood destroying insects. Proceedings of IRG Annual Meeting 1992, Harrogate, UK, IRG/WP 92-2416, 9 pp.
- Fujii, Y., Imamura, Y., Yoshimura, T. (1995) Observation of feeding behavior of termite using CCD camera and its relation to the generation of acoustic emission (AE). *Wood Research* **82**, 47–53.
- Fujii, Y., Noguchi, M., Imamura, Y., Tokoro, M. (1990) Using acoustic emission monitoring to detect termite activity in wood. *Forest Products Journal* **40**(1), 34–36.
- Fujii, Y., Yanase, Y., Imamura, Y., Okumura, S., Oka, S. (1998) Detection of termite attack in wooden buildings with AE monitoring: case study at a traditional Japanese warehouse (in Japanese). *Japanese Journal of Environmental Entomology and Zoology* **9**(3), 101–105.
- Fukuda, K., Otuka, T., Imaizumi, S. (1994) Insect damage of kaya roofing materials and their control method (in Japanese). *Mokuzai Hozon (Wood Protection)* **20**(4), 195–200.
- Garcia, C. M., Morrell, J. J. (2008) Seasonal occurrence of the powderpost beetle, *Dinoderus minutus*, in the Philippines. *Journal of Tropical Forest Science* **20**(2), 139–145.

- Garcia, C. M., Morrell, J. J. (2009) Development of the powderpost beetle (Coleoptera: Bostrichidae) at constant temperatures. *Environmental Entomology* **38**(2), 478–483.
- Garcia, C. M., Morrell, J. J. (2010) Efficacy and economic benefits of prophylactic treatments of newly felled bamboo. *Journal of Economic Entomology* **103**(1), 101–107.
- Himmi, S. K., Yoshimura, T., Yanase, Y., Oya, M., Torigoe, T., Imazu, S. (2014) X-ray tomographic analysis of the initial structure of the royal chamber and the nest-founding behavior of the drywood termite *Incisitermes minor*. *Journal of Wood Science* **60**(6), 453–460.
- Hirano, Y., Shida, S., Arima, T. (2003) Effect of cutting season on biodeterioration in madake (*Phyllostachys bambusoides*) (in Japanese). *Mokuzai Gakkaishi* **49**(6), 437–445.
- Imamura, Y., Adachi, A., Fujii, Y. (1998) Acoustic emission (AE) detected from wood attacked by powder-post beetles, *Lyctus brunneus* STEPHENS (in Japanese). *Japanese Journal of Environmental Entomology and Zoology* **9**(3), 98–100.
- Imamura, Y., Fujii, Y. (1995) Analysis of feeding activities of termites by AE monitoring of infested wood (in Japanese). *Mokuzai Hozon (Wood Protection)* **21**(2), 61–69.
- Indrayani, Y., Nakayama, T., Yanase, Y., Fujii, Y., Yoshimura, T., Imamura, Y. (2003) Feeding activities of the dry-wood termite *Cryptotermes domesticus* (Haviland) under various relative humidity and temperature conditions using acoustic emission monitoring. *Japanese Journal of Environmental Entomology and Zoology* **14**(4), 205–212.
- Indrayani, Y., Yoshimura, T., Yanase, Y., Fujii, Y., Imamura, Y. (2007a) Evaluation of the temperature and relative humidity preferences of the western dry-wood termite *Incisitermes minor* (Hagen) using acoustic emission (AE) monitoring. *Journal of Wood Science* **53**(1), 76–79.
- Indrayani, Y., Yoshimura, T., Yanase, Y., Fujii, Y., Matsuoka, H., Imamura, Y. (2007b) Observation of feeding behavior of three termite (Isoptera) species: *Incisitermes minor*, *Coptotermes formosanus*, and *Reticulitermes speratus*. *Sociobiology* **49**(3), 121–134.
- Iwata, R., Nishimoto, K. (1985) Studies on the autecology of *Lyctus brunneus* (STEPHENS) (Coleoptera, Lyctidae): VI. Larval development and instars with special reference to an individual rearing method. *Wood Research* **71**, 32–45.
- Jennings, J. T., Austin, A. D. (2011) Novel use of a micro-computed tomography scanner to trace larvae of wood boring insects. *Australian Journal of Entomology* **50**(2), 160–163.
- Johnson, J., Marcotte, M. (1999) Irradiation control of insect pests of dried fruits and walnuts. *Food Technology* **53**, 46–51.
- Jones, S. R., Ritchie, P. D. (1937) Radiographic detection of *Lyctus* larvae *in situ*. *Technical Studies in the Field of Fine Arts* **5**(3), 179–181.
- Kamimura, K., Moriyama, Y. (2004) On the household pest control method and IPM (in Japanese). *House and Household Insect Pests* **26**(2), 71–98.
- Kartika, T., Yoshimura, T. (2013) Nutritional quality of diet and fecundity in *Lyctus africanus* (Lesne). *Procedia Environmental Sciences* **17**, 97–104.
- Kawakami, Y., Iwata, R. (1993) *Dinoderus bifoveolatus* (WOLLASTON) (Coleoptera: Bostrychidae) further found in Japan (in Japanese). *House and Household Insect Pests* **15**(1), 17–20.

- Khalil, M. A. K., Rasmussen, R. A., French, J. R. J., Holt, J. A. (1990) The influence of termites on atmospheric trace gases: CH₄, CO₂, CHCl₃, N₂O, CO, H₂, and light hydrocarbons. *Journal of Geophysical Research* **95**(D4), 3619–3634.
- Kigawa, R., Torigoe, T., Imazu, S., Honda, M., Harada, M., Komine, Y., Kawanobe, W. (2009) Detection of insects in wooden objects by X-ray CT scanner (in Japanese). *Science for Conservation* **48**, 223–231.
- Koestler, R. J., Sardjono, S., Koestler, D. L. (2000) Detection of insect infestation in museum objects by carbon dioxide measurement using FTIR. *International Biodeterioration & Biodegradation* **46**(4), 285–292.
- Le Conte, S., Vaiedelich, S., Thomas, J.-H., Muliava, V., de Reyer, D., Maurin, E. (2015) Acoustic emission to detect xylophagous insects in wooden musical instrument. *Journal of Cultural Heritage* **16**(3), 338–343.
- Lemaster, R. L., Beall, F. C., Lewis, V. R. (1997) Detection of termites with acoustic emission. *Forest Products Journal* **47**(2), 75–79.
- Lewis, V. R., Fouche, C. F., Lemaster, R. L. (1997) Evaluation of dog-assisted searches and electronic odor devices for detecting the western subterranean termite. *Forest Products Journal* **47**(10), 79–84.
- Lewis, V. R., Lemaster, R. L. (1991) The potential of using acoustical emission to detect termites within wood. In: M. I. Haverty, W. W. Wilcox (technical coordinators), Proceedings of the symposium on current research on wood-destroying organisms and future prospects for protecting wood in use; Sept. 13, 1989; USDA Forest Service Gen. Tech. Rep. PSW-128. pp. 34–37.
- Lewis, V. R., Lemaster, R. L., Beall, F. C., Wood, D. L. (1991) Using AE monitoring for detecting economically important species of termites in California. Proceedings of IRG Annual Meeting 1991, Kyoto, Japan, IRG/WP 2375, 8 pp.
- Lewis, V. R., Power, A. B., Haverty, M. I. (2004) Surface and subsurface sensor performance in acoustically detecting western drywood termites in naturally infested boards. *Forest Products Journal* **54**(6), 57–62.
- Logan, J. A., Bentz, B. J., Vandygriff, J. C., Turner, D. L. (1998) General program for determining instar distributions from headcapsule widths: example analysis of mountain pine beetle (Coleoptera: Scolytidae) data. *Environmental Entomology* **27**(3), 555–563.
- Matsuoka, H., Fujii, Y., Okumura, S., Imamura, Y., Yoshimura, T. (1996) Relationship between the type of feeding behavior of termites and the acoustic emission (AE) generation. *Wood Research* **83**, 1–7.
- Miyamoto, H. (1985) Insect damage to outside telecommunication plant, especially in electrical cables and wires (in Japanese). *House and Household Insect Pests* (23, 24), 56–68.
- Mori, H., Arai, H. (1979) Insect damage in bamboo materials and its prevention (in Japanese). *House and Household Insect Pests* (1, 2), 9–23.
- Mori, H., Kumagai, M., Hirokawa, K., Machida, K. (1979) Ecological observative method of *Lyctus* powder-post beetles through Roentgenography (in Japanese). *House and Household Insect Pests* (3, 4), 60–73.
- Nagata, S., Morooka, N., Asaoka, K., Nagasawa, H. (2011) Identification of a novel hemolymph peptide that modulates silkworm feeding motivation. *Journal of Biological Chemistry* **286**(9), 7161–7170.

- Nagata, S., Nagasawa, H. (2006) Effects of diet-deprivation and physical stimulation on the feeding behaviour of the larvae of the silkworm, *Bombyx mori*. *Journal of Insect Physiology* **52**(8), 807–815.
- Nair, K. S. S., Mathew, G., Varma, R. V., Gnanaharan, R. (1983) Preliminary investigations on the biology and control of beetles damaging stored reeds. (KFRI Research Report 19), Kerala Forest Research Institute, Peechi, 35 pp.
- NDIS 2110 (1997) Method for measurement of sensitivity degradation of acoustic emission transducer (in Japanese). Japanese Society for Non-Destructive Inspection, Tokyo, Japan.
- Niiho, C. (1984) Ecological study of the tobacco beetle, *Lasioderma serricorne* (F.): II. Growth of tobacco beetles fed on bread crumbs (in Japanese). *Japanese Journal of Applied Entomology and Zoology* **28**(4), 209–216.
- Ninomiya, S., Kotani, K. (2002) Feeding tests by *Dinoderus minutus* Fabricius on acetylated bamboo (in Japanese). *Mokuzai Hozon (Wood Protection)* **28**(4), 135–143.
- Nobuchi, A. (1986) Two new discovered species of Bostrychidae (Coleoptera) from Japan (in Japanese). *Mokuzai Hozon (Wood Protection)* **12**(3), 237–241.
- Nobuchi, A. (1992) Identification for timber pests and their allied insects found in house, II (in Japanese). *Mokuzai Hozon (Wood Protection)* **18**(3), 129–144.
- Noguchi, M., Fujii, Y., Owada, M., Imamura, Y., Tokoro, M., Tooya, R. (1991) AE monitoring to detect termite attack on wood of commercial dimension and posts. *Forest Products Journal* **41**(9), 32–36.
- Norhisham, A. R., Abood, F., Rita, M., Hakeem, K. R. (2013) Effect of humidity on egg hatchability and reproductive biology of the bamboo borer (*Dinoderus minutus* Fabricius). *SpringerPlus* **2**, 9.
- Norhisham, A. R., Faizah, A., Zaidon, A. (2015) Effects of moisture content on the bamboo borer *Dinoderus minutus*. *Journal of Tropical Forest Science* **27**(3), 334–341.
- Okahisa, Y., Azuma, M., Hikita, Y. (2005) A survey on the architectural use of bamboo in Japan (in Japanese). *Mokuzai Hozon (Wood Protection)* **31**(2), 57–62.
- Okahisa, Y., Yoshimura, T., Imamura, Y. (2006) Seasonal and height-dependent fluctuation of starch and free glucose contents in moso bamboo (*Phyllostachys pubescens*) and its relation to attack by termites and decay fungi. *Journal of Wood Science* **52**(5), 445–451.
- Panzavolta, T. (2007) Instar determination for *Pissodes castaneus* (Coleoptera: Curculionidae) using head capsule widths and lengths. *Environmental Entomology* **36**(5), 1054–1058.
- Plank, H. K. (1948) Biology of the bamboo powder-post beetle in Puerto Rico. (Bulletin No. 44), Federal Experiment Station in Puerto Rico, Mayaguez, 29 pp.
- Plank, H. K. (1950) Studies of factors influencing attack and control of the bamboo powder-post beetle. (Bulletin No. 48), Federal Experiment Station in Puerto Rico, Mayaguez, 39 pp.
- Plank, H. K., Hageman, R. H. (1951) Starch and other carbohydrates in relation to the powder-post beetle infestation in freshly harvested bamboo. *Journal of Economic Entomology* **44**(1), 73–75.
- Robbins, W. P., Mueller, R. K., Schaal, T., Ebeling, T. (1991) Characteristics of acoustic emission signals generated by termite activity in wood. Proceedings of IEEE 1991 Ultrasonics Symposium, Orlando, Florida, USA, 1047–1051.
- Saito, T., Matsumoto, Y., Hirashima, Y., Kuno, E., Nakashima, T. (1986) Shin-ōyō-konchū-gaku (Applied entomology: new revision) (in Japanese). Asakura Publishing, Tokyo, p. 121.

- Sanderson, M. G. (1996) Biomass of termites and their emissions of methane and carbon dioxide: a global database. *Global Biogeochemical Cycles* **10**(4), 543–557.
- Schäfer, K., Goergen, G., Borgemeister, C. (2000) An illustrated identification key to four different species of adult *Dinoderus* (Coleoptera: Bostrichidae), commonly attacking dried cassava chips in West Africa. *Journal of Stored Products Research* **36**(3), 245–252.
- Scheffrahn, R. H., Robbins, W. P., Busey, P., Su, N.-Y., Mueller, R. K. (1993) Evaluation of a novel, hand-held, acoustic emissions detector to monitor termites (Isoptera: Kalotermitidae, Rhinotermitidae) in wood. *Journal of Economic Entomology* **86**(6), 1720–1729.
- Simpson, S. J. (1982) Patterns in feeding: a behavioural analysis using *Locusta migratoria* nymphs. *Physiological Entomology* **7**(3), 325–336.
- Sitaraman, N. L. (1951) Studies on the common bamboo-borer, *Dinoderus ocellaris* Steph. Part III. Biology. *Proceedings of the Indian Academy of Sciences - Section B* **34**(3), 148–156.
- Sokolove, P. G., Bushell, W. N. (1978) The chi square periodogram: its utility for analysis of circadian rhythms. *Journal of Theoretical Biology* **72**(1), 131–160.
- Sone, K., Mori, T., Ide, M., Setoguchi, M., Yamanouchi, K. (1995) Application of computer tomography to surveys of the galleries of the oak borer, *Platypus quercivorus* (MARUYAMA) (Coleoptera: Platypodidae) (in Japanese). *Japanese Journal of Applied Entomology and Zoology* **39**(4), 341–344.
- Stušek, P., Pohleven, F., Čapl, D. (2000) Detection of wood boring insects by measurement of oxygen consumption. *International Biodeterioration & Biodegradation* **46**(4), 293–298.
- Sugimoto, A., Inoue, T., Tayasu, I., Miller, L., Takeichi, S., Abe, T. (1998) Methane and hydrogen production in a termite-symbiont system. *Ecological Research* **13**(2), 241–257.
- Suzuki, K., Kirton, L. G. (1991) An evaluation of some cereal and tuber based artificial diets for laboratory culture of *Dinoderus minutus* Fabricius (Coleoptera: Bostrychidae) (in Japanese). *House and Household Insect Pests* **13**(2), 59–65.
- The Society of House and Household Pests Science, Japan (ed.) (1995) Kaoku-gaichū-jiten (Encyclopedia of house and household pests) (in Japanese). Inoue Shoin, Tokyo, 468 pp.
- Tokyo National Research Institute for Cultural Properties (ed.) (2001) Bunkazai-gaichū-jiten (Encyclopedia of insect pests of cultural properties) (in Japanese). Kuba Pro., Tokyo, 231 pp.
- Torigoe, T., Kigawa, R., Harada, M., Komine, Y., Imazu, S., Honda, M., Kawanobe, W. (2010) Investigation of damaged wooden objects and application of X-ray CT to detect insect activity (in Japanese). *Science for Conservation* **49**, 191–196.
- Uchimura, E. (2005) Take to take wo ikasu: take no seitai-kanri to take no riyō (Utilization of bamboo: ecology and management of bamboo plants and use of bamboo materials) (in Japanese). (Ringyō-kairyō-fukyū-sōsho No. 148), Zenrinkyou, Tokyo, 196 pp.
- Uchimura, E. (2012) Take-shigen no shokubutsu-shi (Flora of bamboo resources) (in Japanese). Soshinsha, Tokyo, 241 pp.
- Uchimura, E. (ed.) (2009) Gendai ni ikasu take-shigen (Utilization of bamboo resources in the present day) (in Japanese). Soshinsha, Tokyo, 217 pp.
- Ueda, K. (1963) Useful bamboo and edible sprout (in Japanese). Hakuyusha, Tokyo, 314 pp.

- Watanabe, H., Yanase, Y., Fujii, Y. (2015a) Evaluation of larval growth process and bamboo consumption of the bamboo powder-post beetle *Dinoderus minutus* using X-ray computed tomography. *Journal of Wood Science* **61**(2), 171–177.
- Watanabe, H., Yanase, Y., Fujii, Y. (2015b) Evaluation of larval feeding activity of the bamboo powder-post beetle *Dinoderus minutus* using acoustic emission monitoring. International Symposium on Wood Science and Technology 2015 Abstract Book, Tokyo, Japan, 207.
- Watanabe, H., Yanase, Y., Fujii, Y. (2016) Relationship between the movements of the mouthparts of the bamboo powder-post beetle *Dinoderus minutus* and the generation of acoustic emission. *Journal of Wood Science* **62**(1), 85–92.
- Watanabe, H., Yanase, Y., Fujii, Y. (2017a) Nondestructive evaluation of egg-to-adult development and feeding behavior of the bamboo powderpost beetle *Dinoderus minutus* using X-ray computed tomography. *Journal of Wood Science* **63**(5), 506–513.
- Watanabe, H., Yanase, Y., Fujii, Y. (2017b) Continuous nondestructive monitoring of larval feeding activity and development of the bamboo powderpost beetle *Dinoderus minutus* using acoustic emission. *Journal of Wood Science* doi: 10.1007/s10086-017-1678-4, 11 pp.
- Watanabe, H., Yanase, Y., Fujii, Y. (2017c) Nondestructive analysis of oviposition of the bamboo powderpost beetle *Dinoderus minutus* using acoustic emission and X-ray CT. Proceedings of IRG Annual Meeting 2017, Ghent, Belgium, IRG/WP 17-10889, 8 pp.
- Weissling, T. J., Thoms, E. M. (1999) Use of an acoustic emission detector for locating Formosan subterranean termite (Isoptera: Rhinotermitidae) feeding activity when installing and inspecting aboveground termite bait stations containing hexaflumuron. *Florida Entomologist* **82**(1), 60–71.
- Wood Technological Association of Japan (ed.) (1961) Mokuzai-hozon handbook (Wood protection handbook) (in Japanese). Shokodo, Tokyo, pp. 357–456.
- Wright, C. G. (1960) Biology of the southern lyctus beetle, *Lyctus planicollis*. *Annals of the Entomological Society of America* **53**(3), 285–292.
- Yaghi, N. (1924) Application of the Rontgen tube to detection of boring insects. *Journal of Economic Entomology* **17**(6), 662–663.
- Yamano, K. (1976) Kenchiku-konchū-ki (Insect pests of buildings) (in Japanese). Sagami Shobo, Tokyo, 286 pp.
- Yanase, Y., Fujii, Y., Okumura, S., Imamura, Y., Kozaki, M. (1999) Detection of termite attack in wooden buildings using AE monitoring: a case study at a house of wooden panel construction (in Japanese). *Japanese Journal of Environmental Entomology and Zoology* **10**(4), 160–168.
- Yanase, Y., Fujii, Y., Okumura, S., Imamura, Y., Yoshimura, T. (1998) Detection of AE generated by the feeding activity of termites using PVDF (polyvinylidene fluoride) film. *Forest Products Journal* **48**(7/8), 43–46.
- Yanase, Y., Fujii, Y., Okumura, S., Imamura, Y., Yoshimura, T. (2000a) Plate-type waveguides for detecting acoustic emissions generated by termite attacks. *Journal of Wood Science* **46**(3), 243–247.
- Yanase, Y., Fujii, Y., Okumura, S., Yoshimura, T. (2012) Detection of metabolic gas emitted by termites using semiconductor gas sensors. *Forest Products Journal* **62**(7–8), 579–583.

- Yanase, Y., Fujii, Y., Okumura, S., Yoshimura, T., Imamura, Y. (2000b) Development of AE sensor using PVDF film for detecting termite attack (in Japanese). *Journal of the Society of Materials Science, Japan* **49**(4), 401–405.
- Yanase, Y., Fujii, Y., Okumura, S., Yoshimura, T., Imamura, Y. (2001) Detection of termite attack of *Incisitermes minor* (Hagan) using AE monitoring (in Japanese). *Japanese Journal of Environmental Entomology and Zoology* **12**(2), 53–67.
- Yanase, Y., Maruyama, S., Fujii, Y., Okumura, S., Yoshimura, T. (2013a) Detection of hydrogen and methane emitted by feeding activity of termite under forced ventilation. *Japanese Journal of Environmental Entomology and Zoology* **24**(3), 97–105.
- Yanase, Y., Miura, M., Fujii, Y., Okumura, S., Yoshimura, T. (2013b) Evaluation of the concentrations of hydrogen and methane emitted by termite using a semiconductor gas sensor. *Journal of Wood Science* **59**(3), 243–248.
- Yanase, Y., Mori, T., Yoshimura, T., Fujiwara, Y., Fujii, Y., Torigoe, T., Imazu, S. (2014) Relationship between porosity in wood attacked by the drywood termite *Incisitermes minor* and residual bending strength (in Japanese). *Journal of the Society of Materials Science, Japan* **63**(4), 320–325.
- Yasutomi, K., Umeya, K. (1983) Household pests (in Japanese). Zennokyo, Tokyo, 310 pp.
- Yoshimoto, T., Morita, S. (1985) Studies on hot-water extractives of bamboo stem (*Phyllostachys pubescens* Mazel): seasonal variation of the content of free sugars (in Japanese). *Bulletin of the University of Tokyo Forests* **74**, 9–15.
- Yoshimura, T. (2016) Protection of houses from invasive wood-attacking insects (in Japanese). *Sustainable humanosphere (Japanese ver.)* **12**, 1–10.
- Zimmerman, P. R., Greenberg, J. P., Wandiga, S. O., Crutzen, P. J. (1982) Termites: a potentially large source of atmospheric methane, carbon dioxide, and molecular hydrogen. *Science* **218**(4572), 563–565.